Aus dem Institut für Virologie

der Universitätsmedizin der Johannes Gutenberg-Universität Mainz

The tumor suppressor MYPOP: Characterization of novel MYPOP antibodies and MYPOP application as inhibitor of cell proliferation

Der Tumorsuppressor MYPOP: Charakterisierung neuer MYPOP-Antikörper und Einsatz des MYPOP-Proteins zur Inhibition der Zellproliferation

Inauguraldissertation

zur Erlangung des Doktorgrades der

Medizin

der Universitätsmedizin

der Johannes Gutenberg-Universität Mainz

Vorgelegt von

Sofia-Marie Klemm

aus Laichingen

Mainz, 2024

Wissenschaftlicher Vorstand: Univ.-Prof. Dr. Hansjörg Schild

Tag der Promotion: 30. April 2025

Zusammenfassung

Weltweit sind humane Papillomaviren (HPV) die häufigste sexuell übertragene Infektion (Plotzker *et al.*, 2023), von der im Laufe des Lebens über 80 von 100 Personen in sexuell aktiven Populationen betroffen sind. Insbesondere persistente Infektionen mit Hochrisiko-HPV-Typen bergen ein Krebsrisiko durch virale Onkogene, welche maßgeblich die Transformation der infizierten Zellen bewirken. Trotz der Entwicklung von Impfungen, sind HPV noch für 4,5% der weltweiten Krebsbelastung verantwortlich, darunter oropharyngealer, Gebärmutterhals- und Hautkrebs. Dass Krebserkrankungen die zweithäufigste Todesursache weltweit darstellen und HPV einen signifikanten Anteil davon mitverursachen, verdeutlicht die Wichtigkeit der HPV- und Krebsforschung. Im Allgemeinen wird die Entstehung von Krebs vor allem auf genetische Mutationen zurückgeführt. Mutationen aktivieren Onkogene oder inhibieren Tumorsuppressor-Proteine, wodurch sich Zellen unkontrolliert teilen können. Ein solches Tumorsuppressor-Protein ist MYPOP, welches als Interaktionspartner des kleineren Kapsidproteins L2 von HPV charakterisiert und validiert wurde (Schneider, 2016; Wüstenhagen *et al.*, 2018). MYPOP bindet außerdem HPV-DNA, unterdrückt die virale Transkription und wirkt somit protektiv. Anhand verschiedener Zelllinien konnte gezeigt werden, dass MYPOP in normalen Zellen in gut nachweisbaren Mengen vorliegt, wohingegen es in Tumorzellen verschiedener Krebsarten nicht nachgewiesen werden kann. Darüber hinaus, konnte eine MYPOP Überexpression in diesen Tumorzellen mittels Transfektion eine Reduktion der Zellzahl erreichen (Wüstenhagen *et al.*, 2018). Die Erforschung von MYPOP steckt noch in den Anfängen, weshalb bisher nur wenig Fachliteratur verfügbar ist und weitere Forschungsansätze erforderlich sind. Ziel dieser Arbeit war es deswegen, neue Antikörper und die damit verbundenen Anwendungsmöglichkeiten von MYPOP als Marker für gesundes Gewebes zu testen, sowie Applikationsarten des Proteins auf dem Weg hin zu potenzieller zielgerichteten Krebstherapie zu erproben.

Hierfür wurden monoklonale MYPOP-Antikörper auf den MYPOP Nachweis in normalen Hautzellen, immortalisierten Zellen und Gebärmutterhalskrebszellen getestet. Es konnten drei Antikörper identifiziert werden, die zuverlässig und ohne zusätzliches, unspezifisches Signal, MYPOP detektieren. Sie ermöglichen hier eine Unterscheidung zwischen normalen und immortalisierten Zellen und könnten daher gegebenenfalls diagnostisch eingesetzt werden. Im Vergleich zu den bisher bereits verfügbaren polyklonalen MYPOP Antikörpern konnte eine mindestens gleichwertige Zuverlässigkeit im Western Blot (WB) beobachtet werden.

Auf der Suche nach Applikationsarten von MYPOP mit dem Ziel der Wachstumsreduktion von Krebszellen, schien gereinigtes MYPOP Protein bei direkter Anwendung in der Zellkultur einen möglichen inhibitorischen Effekt vorzuweisen, welcher genauer untersucht werden müsste.

Durch die Produktion und Anwendung von HPV16 PsV wurde zum ersten Mal versucht, MYPOP vektorbasiert als Gentherapie *in vitro* anzuwenden. Dabei wurde zunächst ein erfolgreicher, inhibitorischer Effekt vermutet, der sich bei genauerer Betrachtung dann aber als ein vermutlich auf die Pseudoviren selbst zurückzuführendes Phänomen herausstellte. Da der beobachtete zytotoxische Effekt nur bei Tumor- und nicht bei gesunden Zellen auftrat, sprechen die Ergebnisse trotzdem dafür, diese Beobachtung weiter zu verfolgen. Mit Blick auf aktuelle Ergebnisse der Arbeitsgruppe Florin kann geschlussfolgert werden, dass das MYPOP Protein selbst die Problematik bei der Herstellung der Pseudoviren darstellt. Durch seine antiviralen Eigenschaften interagiert es wahrscheinlich mit Kapsidproteinen oder der zu verpackenden DNA und verhindert die effiziente Verpackung oder Transkription des Expressionsplasmids. Dieses Problem müsste in der zukünftigen Herstellung von MYPOP Pseudoviren berücksichtigt werden.

Zusammenfassend zeigt diese Arbeit geeignete monoklonale MYPOP Antikörper für die zukünftige Produktion und Anwendung in Forschung und möglicher Diagnostik auf. Des Weiteren leistet dieses Projekt einen Beitrag auf dem Weg hin zu einer möglichen therapeutischen Anwendung von MYPOP in der Krebstherapie, indem erstmals die vektorbasierte Transduktion als Applikationsart getestet wird und damit einhergehende Probleme der Virenpräparation dargelegt werden.

Abstract

Globally, human papillomaviruses (HPV) are the most common sexual infection (Plotzker *et al.*, 2023), affecting over 80 out of 100 people in sexually active populations over the course of their life. Infections with high-risk HPV types imply a cancer risk due to viral oncogenes that transform infected cells. Despite the development of vaccines, HPV still account for 4.5% of the global cancer burden, such as oropharyngeal, cervical, and different types of skin cancers. Given that cancer is the second leading cause of death worldwide and HPV plays a significant role in its development, the importance of research on HPV and cancer is undeniable. Generally, cancer onset is attributed above all to genetic mutations. These mutations result in activated oncogenes or non-functional tumor suppressor proteins, enabling cells to divide uncontrollably. One of these tumor suppressor proteins is MYPOP, an interaction partner of the smaller capsid protein L2 of HPV (Wüstenhagen *et al.*, 2018). MYPOP also binds HPV DNA, suppresses viral transcription, and thus exerts a protective effect in the human cell. Various normal cell lines have a well detectable amount of MYPOP. However, it is not detectable in immortalized or tumor cells of different cancer types. Moreover, overexpression of MYPOP in these tumor cells through transfection has been shown to provoke reduction of cell counts (Wüstenhagen *et al.*, 2018). Due to the recent research on MYPOP, the knowledge in the literature is very limited and further research approaches are needed. For this reason, the objective of this project was to test new MYPOP antibodies and their application as markers of healthy tissue and explore ways of using MYPOP for potential targeted cancer therapy.

First monoclonal MYPOP antibodies were tested on normal skin cells, immortalized cells, and cervical cancer cells. In these experiments, three antibodies were identified that reliably differentiate between normal and immortalized cells based on MYPOP expression, which implies a potential use in diagnostics. Compared to the available polyclonal MYPOP antibodies, at least equivalent reliability in Western blot (WB) analyses was observed.

In the search for appropriate applications of MYPOP with the aim of reducing growth of cancer cells, directly applied purified MYPOP protein appeared to exhibit an inhibitory effect, which warrants further detailed investigation. For the first time, MYPOP was attempted to be applied as vector-based gene therapy *in vitro* using HPV16 pseudovirus (PsV). Initially, a successful inhibitory effect was suspected, but it turned out to be a phenomenon rather attributable to the PsV themselves. As the observed cytotoxic effect occurred only in tumor and not in healthy cells, the results still advocate for further exploration. The inclusion of recent findings of the Florin group leads to the assumption that the MYPOP protein itself poses challenges in the production of the PsV. Due to its antiviral properties, it likely interacts with capsid proteins or the DNA to be packaged and prevents efficient packaging or transcription of the expression

plasmid. This issue should be considered and addressed in the future production of MYPOP PsV.

In summary, this work identifies suitable monoclonal MYPOP antibodies for future production and application in research and potential diagnostics. In addition, this project contributes to the path towards a potential therapeutic application of MYPOP in cancer therapy, testing vector-based application and highlighting issues to be considered in MYPOP-vector preparation.

Table of contents

Zusammenfassung I

Abstract III

List of abbreviations VIII

List of figures X

List of tables XI

1 Introduction 1

2 Discussion of literature 3

2.1 Human papillomavirus (HPV) 3

2.1.1 Structure of HPV 4

2.1.2 Infection and viral replication cycle 5

2.1.3 Carcinogenesis of HPV 6

2.2 General carcinogenesis 7

2.3 MYB-related protein, partner of profilin (MYPOP) 9

2.3.1 Structure and function 9

2.3.2 MYPOP antibodies (Abs) 12

2.4 Vector-based gene therapy as cancer treatment approach 12

3 Materials 14

3.1 Laboratory equipment 14

3.2 Consumables 15

3.3 Chemicals, kit systems and reagents 15

3.4 Buffers and solutions 16

3.5 Plasmids 18

3.6 siRNA 18

3.7 Antibodies 18

3.7.1 Primary antibodies 19

3.7.2 Secondary antibodies 19

3.8 Cell culture 19

3.8.1 Cell lines 19
3.8.2 Cell culture media and additives 20
4 Methods 22
4.1 Cultivation of human adherent cells 22
4.1.1 Cultivation of immortalized and cancer cell lines 22
4.1.2 Cultivation of primary keratinocytes (NHEK) 22
4.1.3 Cell stock storage 23
4.2 Production of MYPOP-HPV16 pseudoviruses (MYPOP PsV) 23
4.3 Determination of cell number 24
4.4 DNA and siRNA transfection 25
4.5 Sodium Dodecyl Sulfate Polyacrylamide Gel Electrophoresis 26
4.6 Western Blot (WB) 27
4.7 Immunofluorescence microscopy 28
4.8 Statistics 29
5 Results 30
5.1 Putative MYPOP antibodies as diagnostic tool 30
5.1.1 Polyclonal antibodies detecting MYPOP differ in their signal patterns 30
5.1.2 New MYPOP antibodies show large differences in specificity 31
5.1.3 Identification of a suitable monoclonal MYPOP antibody 33
5.2 Testing of MYPOP protein application to reduce cancer cell growth 35
5.2.1 Elution buffer used for protein purification shows cytotoxic effect 35
5.2.2 Application of purified MYPOP indicates reduction of cell growth 36
5.3 Preparation of HPV16 pseudoviruses (PsV) as viral vectors 37
5.4 Analysis of MYPOP transduction 38
5.4.1 MYPOP-wt PsV reduces cell counts in HeLa 38
5.4.2 MYPOP-wt PsV treatment shows concentration-dependent effect 39
5.4.3 MYPOP is detectable in HeLa and NHEK after transduction 40
5.4.4 Transduction of MYPOP-wt PsV in HeLa cells is moderately efficient 41

5.4.5 MYPOP-wt does not show a typical expression pattern post transduction 42
5.4.6 L1 is not detectable in MYPOP-AD PsV preparation 43
5.5 Follow-up experiments with new PsV 44
5.5.1 MYPOP-AD PsV treatment shows growth reducing effect in cervical cancer cell line HeLa 44
5.5.2 PsV show growth reducing effect in lung cancer cell line A549 45
6 Discussion 47
6.1 Methodological remarks 47
6.2 Polyclonal antibodies detect multiple MYPOP forms 48
6.3 Good prospects for monoclonal MYPOP antibodies 49
6.4 Evaluating the inhibitory effect of purified MYPOP application on cell growth 50
6.5 Evaluation of PsV preparation and MYPOP transduction 51
6.5.1 Defective MYPOP-AD PsV preparation 52
6.5.2 Pseudoviral effect in HeLa and lung cancer cells 53
6.5.3 Problems in vector-based MYPOP gene transduction 54
6.6 Conclusion and future directions 56
7 References 58
Appendix XIII
Acknowledgments XVI

List of abbreviations

Ab	antibody
AD	activation domain
APS	ammonium persulfate
bp	base pair
BSA	bovine serum albumin
CDK	cyclin dependent kinase
Csi	control siRNA
ddH_2O	double-distilled water
DDR	DNA damage-response
DMEM	Dulbecco's Modified Eagle Medium
DMSO	dimethyl sulfoxide
DNA	deoxyribonucleic acid
EDTA	ethylenediaminetetraacetic acid
EMT	epithelial-mesenchymal transition
et al.	*et alia*, [and others]
FCS	fetal calf serum
HaCaT	immortalized Human Keratinocyte *(cell line)*
HeLa	*cell line*, named after Henrietta Lacks, patient with cervical carcinoma
HEK	*cell line* from Human Embryonic Kidney cells
HEPES	4-(2-hydroxyethyl)-1-piperazineethanesulfonic acid
HPV	human papillomavirus(es)
HRP	horse radish peroxidase
IF	Immunofluorescence
LCR	long control region
mAb	monoclonal antibody
MYPOP	MYB-related protein, partner of profilin
NB	nuclear body
NES	nuclear export signal
NHEK	normal human epidermal keratinocytes *(primary cells)*
NLS	nuclear localization signal
ORF	open reading frame
ori	origin of replication
PAGE	polyacrylamide gel electrophoresis
PBS(-T)	phosphate buffered saline (+ 0.1% Tween® 20)
PEI	Polyethylenimine

PML	promyelocytic leukemia protein
PsV	pseudovirus(es)
PTM	post-translational modification
RB	retinoblastoma
rpm	rounds per minute
SDS	sodium dodecyl sulfate
siRNA	small interfering RNA
STD	sexually transmitted disease
TEMED	Tetramethylethylenediamine
TF	transcription factor
VLP	virus-like particle
WB	Western blot
wt	wild type

List of figures

Figure 1: Papillomavirus capsid 4

Figure 2: Genome structure of HPV16 5

Figure 3: Phases of the cell cycle 8

Figure 4: Schematic overview of human MYPOP 10

Figure 5: Schematic representation of FLAG-MYPOP-wt and FLAG-MYPOP-AD 18

Figure 6: Threshold adaptation for determination of cell number 25

Figure 7: Polyclonal antibodies detect endogenous MYPOP expression in NHEK 30

Figure 8: Monoclonal and polyclonal MYPOP antibodies detect purified MYPOP protein 31

Figure 9: Detection pattern of monoclonal MYPOP Abs on HeLa, HaCaT and NHEK cells 32

Figure 10: Further subcloned mAbs detect overexpressed and endogenous MYPOP in WB analysis 34

Figure 11: Elution buffer shows cytotoxic effect 36

Figure 12: Purified MYPOP in elution buffer reduces cell counts in HeLa 37

Figure 13: MYPOP detection in cells treated with peak fractions of the PsV gradients. 38

Figure 14: MYPOP-wt PsV reduces cell counts in HeLa 39

Figure 15: MYPOP-wt PsV shows a concentration-dependent growth inhibitory effect on HeLa cells. 40

Figure 16: FLAG-MYPOP expression in HeLa and NHEK after transduction 41

Figure 17: MYPOP-wt expression in HeLa cells after transduction 42

Figure 18: MYPOP-wt localization in HeLa after transduction 42

Figure 19: Missing L1 signal in MYPOP-AD preparation 43

Figure 20: MYPOP-AD PsV treatment reduces cell growth in HeLa cells 45

Figure 21: PsV treatment reduces cell growth in lung cancer cell line A549. 46

List of tables

Table 1: Laboratory equipment 14
Table 2: Films and membranes 15
Table 3: Chemicals, kit systems and reagents 15
Table 4: Buffers and solutions 16
Table 5: Plasmids 18
Table 6: siRNA 18
Table 7: Primary antibodies 19
Table 8: Secondary antibodies 19
Table 9: Cell lines 19
Table 10: Additional cell lines of the follow-up experiments 20
Table 11: Cell culture media and additives 20

1 Introduction

The family of human papillomaviruses is widespread and known, among other things, to cause tumors. Depending on the subtype, the extent varies from genital warts up to cancer. This relevance has been highlighted by Harald zur Hausen, who received the Nobel Prize in 2008 for discovering that HPV can induce cervical cancer, one of the top five most prevalent cancer types affecting people with uterus in the world (zur Hausen, 1976). Particularly the high-risk types 16 and 18 of HPV can disrupt the host cells normal control of cell division. Expression of HPV oncogenes E6 and E7 promote inactivation of tumor suppressors which is part of the mechanism leading to uncontrolled cell growth (Scheffner and Whitaker, 2003). This can result in the development of cervical, anal, oropharyngeal, and other cancer types, emphasizing the importance of research on HPV infections (zur Hausen, 2009).

Exploring HPV, the Florin group focuses on the mostly unknown protein MYPOP. As a natural restriction factor, MYPOP usually is ubiquitously expressed in human cells. It was discovered that MYPOP levels in HPV-transformed cell lines are significantly decreased and so might be the case in other, non-virally induced cancer types (Wüstenhagen *et al.*, 2018). Following this hypothesis, MYPOP could be valuable as a biomarker distinguishing normal from tumor tissue. Furthermore, MYPOP has been overexpressed in HPV-transformed tumor cell lines by transfection of a MYPOP expression plasmid, which lead to an inhibition of cell growth (Wüstenhagen *et al.*, 2018). This suggests the potential for (re-)expressing MYPOP in tumor cells as a cancer therapy.

To this day, medical treatments of cancer are limited and mostly imply serious side effects (Mukherjee, 2010). In various cases not only surgery, but also systemic chemotherapeutical treatment or radiation is needed. These traditional approaches in particular are associated with a variety of serious side effects. New methods like hormone therapy, immunotherapy, targeted therapy, and gene therapy have been developed over the last decades and are among others also used in cancer therapy. They are designed to be more selective, aiming to both increase effectiveness and minimize damage to normal cells (Schirrmacher, 2019).

Gene therapy is one of these new medical approaches. It involves the introduction of genetic material into a person's cells to treat or prevent disease (Weichselbaum and Kufe, 1997). The process can involve the use of vectors, such as viral vectors, to deliver therapeutic genes into target cells. Viral vectors are modified viruses transporting genetic material without the ability of causing disease. There are a variety of viral vector systems, based on different types of viruses. The most well-known are derived from adenoviruses or lentiviruses (Chen, Keiser and Davidson, 2018). One promising vector system is HPV16-based and exhibits a preference to bind to tumor cells (Kines *et al.*, 2016).

The aim of this project, in connection with the need for new targeted cancer therapies, is to further characterize MYPOP's potential as a normal tissue marker on the one hand and as tumor suppressor and potential candidate for gene therapy on the other. The following questions are addressed:

- Is there a monoclonal MYPOP antibody that can distinguish normal from tumor tissue?
- Does direct MYPOP protein application inhibit cell growth of tumor cells?
- Is transduction with human papillomaviral vectors a suitable approach for a possible future therapeutic use of MYPOP?
- Does MYPOP re-/overexpression affect normal, non-tumor cells?

To this end, the first part of this thesis contributes to the development of MYPOP antibodies as a potential diagnostic tool by identifying a monoclonal antibody that can differentiate normal from tumor tissue based on different MYPOP expression levels. The tested monoclonal antibodies were generated in a collaborative project involving expertise in antigen production (Florin group) and antibody production including immunization of mice (DKFZ Heidelberg). The second part of the project deals with the potential therapeutic benefit of the protein MYPOP: On the one hand, direct application of MYPOP and on the other hand, transduction of its expression plasmid through viral vectors (HPV16 PsV) is explored. In this way, two possible, so far untested, application strategies of MYPOP and their effects on normal and tumor cells are analyzed.

2 Discussion of literature

2.1 Human papillomavirus (HPV)

Human papillomavirus (HPV) represents a diverse group of small, non-enveloped double-stranded DNA viruses that infect epithelial cells of the skin and mucosa in humans. With currently over 200 identified types (International HPV Reference Center, IHRC, 2023) (Bernard *et al.*, 2010), HPV comprises varying degrees of clinical significance, from asymptomatic infections to the development of cancer (Bravo and Félez-Sánchez, 2015; zur Hausen, 2001). This diversity is thought to be due to their focus on different ecological niches in their development over the years (Van Doorslaer, 2013).

HPV is the most common sexually transmitted infection worldwide, affecting over 80 out of 100 persons in sexually active populations during their lifetime. (Da Ros and Schmitt Cda, 2008; Plotzker *et al.*, 2023; Chesson *et al.*, 2014). While most HPV infections are transient and asymptomatic, high-risk genotypes like 16, 18, 31 and 45 have been labeled oncogenic and linked to the development of a range of malignancies, most notably cervical cancer (Araldi *et al.*, 2018). In 2008, zur Hausen received the Nobel Prize for discovering that HPV can cause cervical cancer (zur Hausen, 1976). Since then, the first virally induced cancer to be discovered has been studied. It has been associated with a variety of origin tissues. Apart from the cervix, precancerous and manifest HPV-related cancer has been detected, among others, in anogenital tissues (Serrano *et al.*, 2015), head and neck (Major *et al.*, 2005), breast (Islam, Chakraborty and Panda, 2020), esophagus (Syrjänen, 2002) and skin (Lambert *et al.*, 2020; zur Hausen, 2009). In HPV-associated cancer, HPV16 is usually detected most frequently, followed by type 18 (zur Hausen, 2009), which is why this work focuses on cell lines transformed by these two genotypes.

Recognition that a virus causes a significant cancer burden has become a central issue in preventive medicine, and several effective vaccines against the most oncogenic HPV genotypes have been developed (Bergman *et al.*, 2019). Vaccination campaigns demonstrated substantial reductions in the prevalence of infections (Saraiya *et al.*, 2015), offering promise for long-term reductions in HPV-related cancer incidence. However, HPV-associated cancer remains a significant health burden, accounting for 4.5% of the global cancer rate (de Martel *et al.*, 2017), particularly in regions where access to healthcare, health education and HPV vaccination or its coverage remain limited. These challenges, together with the existence of non-vaccine HPV genotypes (Choi *et al.*, 2012) demonstrate the necessity of public health efforts and ongoing research.

2.1.1 **Structure of HPV**

HPV are small non-enveloped DNA viruses with a diameter of 55 - 60 nm (Wang and Roden, 2013). The icosahedrally shaped capsid is formed by the two structural proteins, L1 and L2. L1, the major capsid protein, occurs 360 times per virus and is assembled into 72 pentamers. The minor capsid protein L2 can occur up to 72 times, interacts with the pentamers and the virus genome and plays a role in the viral assembly (Baker *et al.*, 1991; Wang and Roden, 2013).

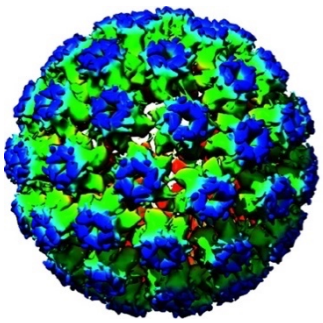

Figure 1: Papillomavirus capsid
Modified cryo-EM structure of an HPV16 capsid at 4.5 Å resolution (from: Van Doorslaer *et al.*, 2018). The structure of the L1 pentameters can be seen in blue-green coloration.

In contrast to L2, L1 has the ability to self-assemble and in this way form virus-like particles (VLPs) that are the basis for the licensed HPV vaccines (Kirnbauer *et al.*, 1992; Buck, Day and Trus, 2013). Expression of both structural proteins in combination can be used to encapsulate desired DNA within the original viral capsid to produce PsV (Buck *et al.*, 2004).

Packed in the capsid, HPV have double-stranded DNA genomes of about 8,000 bp that are arranged circularly and condensed by histones (de Villiers *et al.*, 2004). A representative HPV genome is given in Figure 2. Each genome can be divided into different parts: The *early region* contains the open reading frames (ORFs), which encode the proteins E1-7. E1 and E2 are two regulatory proteins involved in transcriptional and replicational processes (Egawa *et al.*, 2012; McBride, 2013). E4 can vary between different HPV types and contributes for instance to amplify the genome or viral synthesis (Doorbar, 2013). E5, E6, and E7 promote cell division of the host cell through apoptosis modulation and especially E6 and E7 have been discovered to be potent oncogenes (Skelin, Sabol and Tomaić, 2022). The *late region* encodes the capsid proteins L1 and L2. Between the *late* and *early region*, the *long control region* (LCR) is located. It contains the *origin of replication* (ori) and most cis-responsive elements, which are specific DNA sequences regulating gene expression. In general, the ORFs of the proteins are well conserved among the virus family, especially those of E1, E2, L1 and L2. In contrast, the LCR is poorly conserved (de Villiers *et al.*, 2004).

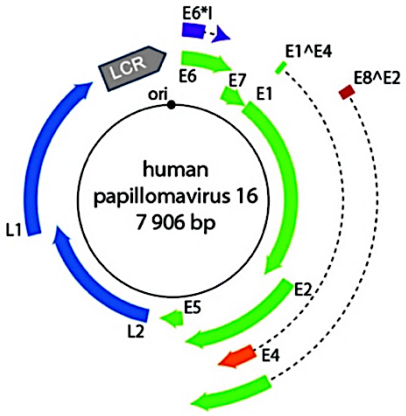

Figure 2: Genome structure of HPV16
Schematic overview of the HPV16 genome and its protein-coding open reading frames (ORFs) (adapted from: Van Doorslaer *et al.*, 2018). ORFs are indicated as colored arrows and labeled with the protein, they encode for. Dotted parts are intron sequences. The viral origin of replication is marked in black (ori).

2.1.2 **Infection and viral replication cycle**

Viruses have no metabolic capability of their own and therefore rely on host cells to replicate. Since infection of cervical tissue is best studied, this host cell type is used to describe the replication of HPV. Its life cycle is tightly intertwined with the differentiation program of host epithelial cervix cells and is not yet understood in every detail (Doorbar *et al.*, 2015). Apparently, HPV gene transcription can only be started in host cells progressing through the cell cycle for division (Pyeon *et al.*, 2009). Regarding skin and mucosa, this only applies to the basal cells. Reaching this dividing layer represents an obstacle for HPV, which is why at least micro wounds are thought to be obligatory for HPV infection (DiGiuseppe *et al.*, 2017). For viral entry into cells, L1 interacts with structures of the extracellular matrix, precisely heparan sulfate proteoglycans (Joyce *et al.*, 1999; Giroglou *et al.*, 2001). Conformational processes set in motion include both structural “L” proteins and result in the exposure of the L2 N-terminus, which starts proteolytic changes (Bienkowska-Haba, Patel and Sapp, 2009). The affinity for heparan sulfate proteoglycans decreases and endocytosis occurs with involvement of other receptor types such as integrins (Evander *et al.*, 1997) and tetraspanins (Spoden *et al.*, 2008; Scheffer *et al.*, 2013). Tetraspanins play a crucial role by forming tetraspanin-enriched microdomains in the plasma membranes of the cells, which are likely to act as entry platforms (Scheffer, Berditchevski and Florin, 2014). Finally, the involvement of the actin cytoskeleton leads to the endocytosis of the viruses along with the secondary receptor complexes (DiGiuseppe *et al.*, 2017; Spoden *et al.*, 2013). Once internalized, uncoating of HPV begins probably triggered by acidification and cellular proteins in the endosomes. The majority of L1 proteins detach and the conformational changes allow the remaining complex, consisting of L2 and the viral genome, to gain contact with the cytoplasm via the C-terminal side of L2. Through interaction with cellular proteins such as nexins, dynein, and mitotic chromatin viral

transport towards the trans-Golgi network and subsequently the nucleus takes place (Müller *et al.*, 2014; Bienkowska-Haba *et al.*, 2012; Mikuličić, Strunk and Florin, 2021). This migration is microtubule-dependent, and minus-end-directed (Florin *et al.*, 2006). Through binding to condensed chromosomes during mitosis, the HPV-containing vesicles become internalized in the nuclear membrane at its reorganization (DiGiuseppe *et al.*, 2016). In the nucleus, the viral genome is released and accumulates with, among others, promyelocytic leukemia protein (PML) nuclear bodies (NB) (Mikuličić, Strunk and Florin, 2021). PML NB exert effects on incoming DNA viruses, such as an antiviral effect on Herpes simplex virus (Komatsu, Nagata and Wodrich, 2016). For HPV, they are thought to act as promoters of successful infection and the start of transcription (Day *et al.*, 2004). Initial transcription and maintenance of replication of the HPV genome is additionally promoted by the early proteins E1 and E2 and recruitment of the DNA damage-response (DDR) system for viral replication (Gillespie *et al.*, 2012; Sakakibara, Mitra and McBride, 2011). Interaction with host cell chromatin assures viral dissemination. When dividing asymmetrically, the viral genome passes on to both a new basal cell (as a persistent infection) and a new differentiating cell (so that effective viral amplification can take place). The more differentiated the cells become, the higher the viral amplification rate is (McBride, 2008). The diverse viral proteins, listed in 2.1.1, are progressively synthesized and exert their respective roles in maintaining viral replication, creating the best conditions in the host cell, promoting cell division, and ultimately assembling new viruses. L1 and L2, the late proteins, are synthesized in the upper layers of the epithelium, respectively, and serve as packaging for new virus particles that are subsequently shed from the surface (McBride, 2017).

During its life cycle and especially on its way from cell surface to nucleus and start of transcription, the virus needs to overcome different cellular anti-viral defense mechanisms. There is a variety of cell structures acting anti- or pro-viral concerning HPV (Mikuličić, Strunk and Florin, 2021). One pro-viral example is p62, which accompanies L2 and the viral DNA to the PMLs, forming virus-p62-PML hybrid bodies. It represses autophagy and allows viral gene transcription (Schweiger *et al.*, 2022). An example of an antiviral cell protein is the transcription factor MYPOP. It has been uncovered among other to repress early gene expression of the high-risk types 16 and 18 (see also chapter 2.3, Wüstenhagen *et al.*, 2018; Strunk *et al.*, 2024).

2.1.3 **Carcinogenesis of HPV**

High-risk HPV genomes can be found in more than 99% of cervical cancer biopsies (Forman *et al.*, 2012; Cancer Research CancerResearchUK, 2024 statistics, 2024) and are known to contribute essentially to its development (zur Hausen, 2009). Infection with HPV is very common, as mentioned above. To develop cancer or precancerous transformations, however, persistence of a high-risk type infection is necessary, which occurs in less than 10% (Schiffman

et al., 2007). Normally, the viral genome reproduces outside the host cell genome in a so-called replicon. In cells that have evolved into cancer, the viral genome can often be found integrated into the host cell genome (Schwarz *et al.*, 1985; Adey *et al.*, 2013). This is not a regular part of the replication cycle and is not useful to produce packable viral genomes, which is why the reason for DNA integration remains unclear. So far, it is attributed to the localization of the viral genome replication at fragile host DNA loci, where the exploited DDR system potentially integrates viral DNA during its repair processes (Jang, Shen and McBride, 2014). Integration of viral DNA is thought to lead to dysregulated expression of viral oncogenes E6 and E7 (Jeon, Allen-Hoffmann and Lambert, 1995; McBride, 2022). The two oncogenic proteins bind protective factors or promote their degradation by interacting via the ubiquitin-proteasome system. E6 binds and promotes the degradation of the tumor suppressor p53, inhibits cellular terminal differentiation, and induces immortalization. E7 targets members of the growth-repressive retinoblastoma (RB) family and the restriction factor MYPOP (Scheffner and Whitaker, 2003; Scheffner *et al.*, 1990; Nominé *et al.*, 2006; McBride, 2022). E5, in contrast, is attributed a smaller role, promoting carcinogenesis by interaction with growth factor receptors, but not provoking cell transformation (Skelin, Sabol and Tomaić, 2022). Above all, the increased E6 and E7 high-risk protein expression leads to higher division rates, subsequently causing the accumulation of genetic alterations and cancer as a long-term result (Isaacson Wechsler *et al.*, 2012; Jeon, Allen-Hoffmann and Lambert, 1995; Skelin, Sabol and Tomaić, 2022).

2.2 General carcinogenesis

Cancer can start in almost any tissue of the human body. It is characterized by abnormal cells that divide uncontrollably and grow destructively. Additionally, it can spread to other parts and organs of the body (metastasis), which is often the main reason for a lethal prognosis and contributes enormously to global mortality. The relevance of cancer is highlighted by the fact that, today, cancer is the second most common cause of death worldwide with constantly growing prevalence rates (WHO, 2023).

Research on the origin of cancer points towards the mechanism of the cell cycle including cell division and its control, as an underlying cause. The cell cycle is a series of events that a eukaryotic cell goes through during its lifetime (Figure 3). The cell cycle is characterized by three main distinct phases: (i) the interphase, where the cell prepares for division or exits the cycle for resting (G0); (ii) mitosis, in which the cell's genetic material is duplicated and the nuclear envelope breaks down (prophase), the chromosomes align (metaphase), sister chromatids of each chromosome are pulled apart toward opposite poles of the cell (anaphase), and new nuclear envelopes form around the separated chromatids (telophase); (iii)

cytokinesis, where the rest of the cellular components are distributed between two newly formed cells. As a result of the cell cycle, two genetically identical daughter cells are formed (Fior R., 2019).

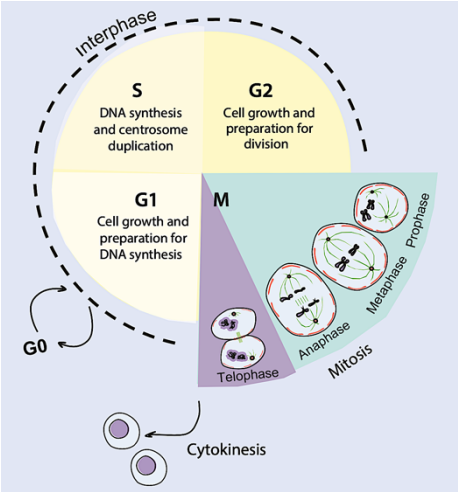

Figure 3: Phases of the cell cycle
Schematic overview of the different phases of the cell cycle: Interphase consisting of G1, S and G2, M = mitosis, cytokinesis. G0= cell exits the cycle for resting. The picture was used from Fior and Zilhao 2019 (Fior R., 2019).

The fundamental biological process of cell division serves two primary functions: On the one hand, it enables an organism to grow to its mature size by increasing the number of cells. On the other hand, it serves in tissue repair and therefore in the maintenance of the adult organism. Hence, the correct course of this process is fundamental for the respective organism and is therefore regulated very precisely. Cyclins in combination with cyclin-dependent kinases (CDKs) are the main regulatory elements, enabling the cell to progress to the next steps during the cell cycle (Fior R., 2019). Increasing levels of a distinct cyclin lead to the activation of associated CDKs, which phosphorylate substrates and induce a signaling cascade that is necessary for the corresponding subphase. A dysregulation of cyclins or CDKs can provoke an early entry into mitosis, resulting in genetic errors through premature cell division (Wood and Endicott, 2018). In addition to positive progression signals, there are also inhibitory influences on the cell cycle to avoid its progression when genomic aberrances are detected. Controls take place at so-called cell cycle checkpoints, where the cell conditions and the genetic material are checked (Fior R., 2019). Detected DNA alterations lead to cell cycle arrest and the promotion of repair mechanisms. When the damage is considered irreparable, programmed cell death (apoptosis) is initiated (Xu, Lai and Hua, 2019).

Various mechanisms can interfere with this complex, genetically defined control system of the human cell cycle, only outlined here. As a result, mutations in the DNA can lead to uncontrolled cell division. Research correlating age and cancer incidence leads to a hypothesis that with increased age, the risk for cancer rises. This suggests that the accumulation of such mutations

is necessary for cancer formation, rather than one single mutation. Following a mathematical model, at least six mutations in combination were thought to be necessary to enable cells to divide in an uncontrolled manner (Armitage and Doll, 1954; Nordling, 1953). Following this assumption, further research on the required number of alterations or affected pathways supports the notion that for cancer development to progress into advanced solid tumors only three mutations in necessary driver genes are sufficient. Driver genes are, in contrast to many accompanying other mutations in tumors, the ones that guarantee a growth advantage (Tomasetti *et al.*, 2015). Due to the advance of genome-wide sequencing technologies, it has been shown that about 200 of 20,000 human genes act as so-called driver genes in the development of frequent cancers. These genes, in turn, influence a limited amount of signal cascades determining the life paths of cells (Vogelstein and Kinzler, 2015).

Driver genes in cancer can be divided into two groups: On the one hand, activated oncogenes result in the overstimulation of proliferation processes such as the CDK pathways. Common oncogenic representatives are RAS, c-MYC, and c-MYB (cellular) as well as E6 and E7 (viral). (Crawford and Tommasino, 1997; Rodenhuis and Slebos, 1992). On the other hand, inactivated (mutation) or destabilized (regulatory mechanisms) tumor suppressors like p53, pRB, or MYPOP fail to regulate various cellular protection mechanisms, such as the above-mentioned cell cycle control, DNA repair, or apoptosis (Bensaad and Vousden, 2005; Mandigo *et al.*, 2022; Wüstenhagen *et al.*, 2018; Strunk *et al.*, 2024).

To sum up, the development of cancer comprises a large field of mechanisms, such as driver gene mutations and destabilization of tumor suppressor proteins. Therefore, it is of great interest to detect and address them specifically for therapeutic approaches (Hu *et al.*, 2021).

2.3 MYB-related protein, partner of profilin (MYPOP)

2.3.1 Structure and function

A recently discovered tumor suppressor is the MYB-related transcription factor MYPOP (human protein). Not only cell division, but the whole cell metabolism is controlled by gene expression. A complex mechanism, in which transcription factors (TFs) play a crucial role in transcription activation, transcription repression, or even both. Mostly, they possess an activation domain (AD) and a DNA-binding domain. By the sequence of the latter, TFs can be divided into sequence-specific groups (Vaquerizas *et al.*, 2009) like the Myb transcription factor family. This family is present in different organisms, with many genes in plants and significantly fewer members in animals (Dubos *et al.*, 2010; Feller *et al.*, 2011). The name of this family derives from v-Myb, the first representative gene of this group. It is a **v**iral oncogene of a retrovirus known as the avian **my**elo**b**lastosis virus. This retrovirus can cause cancer in birds,

specifically in the myeloid cells of the bone marrow, leading to the development of myeloblastosis, a form of leukemia (Klempnauer, Gonda and Bishop, 1982). The v-Myb gene encodes a protein with the specific DNA-binding domain called Myb domain (Biedenkapp *et al.*, 1988; Rosinski and Atchley, 1998). v-Myb is derived from the cellular c-Myb (or MYB in humans), which is the best-studied gene of the family so far. It can be found in the genomes of humans and many other organisms. Moreover, it is involved in the regulation of cell growth, differentiation, and the development of blood cells (Klempnauer *et al.*, 1983). Under certain circumstances, it can act as an oncogene (Zhou and Ness, 2011). For instance it has been discovered that c-Myb specifically binds to an HPV16 enhancer and thereby promotes early oncogene expression of HPV (Nürnberg *et al.*, 1995).

Myb proteins, such as c-Myb, typically possess one to three repeats of the Myb helix-turn-helix DNA-binding domain (R1, R2, R3). Each repeat consists of 51 or 52 amino acids forming three alpha-helices (Ogata *et al.*, 1992). Myb-related proteins also possess the Myb DNA-binding domain, which enables them to bind to Myb-specific DNA sequences and regulate gene transcription. However, variations in the number of repeats or amino acid sequence motifs, compared to Myb proteins like c-Myb, occur.

One of these Myb-related proteins is Mypop (Myb-related protein, partner of profilin), discovered for the first time as the murine version $p42^{POP}$ (Lederer, Jockusch and Rothkegel, 2005). Focusing on profilin, an actin-binding protein involved in cytoskeletal processes, Lederer and his colleagues found $p42^{POP}$ (= murine Mypop) with a yeast two-hybrid system screening as an interaction partner of profilin. Due to its N-terminal DNA-binding domain, which is similar to the Myb domain but with only one repeat, they categorized it as a Myb-related protein. In this so far only publication dedicated to the specific mouse protein, the presence of the Mypop mRNA was found in all mouse tissues, with especially high concentrations in the brain and testis. According to Lederer et al., $p42^{POP}$ is located mainly in the nucleus. It comprises different domains like the DNA binding domain, motifs for nuclear import (NLS) and export (NES), and a leucine zipper, presumably for dimerization. In the nucleus, $p42^{POP}$ represses transcription and is regulated by profilin. The human version of $p42^{POP}$, called MYPOP, was described for the first time in the master's thesis of E. Wüstenhagen and is represented in Figure 4.

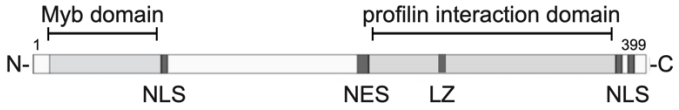

Figure 4: Schematic overview of human MYPOP
MYPOP consists of 399 amino acids, containing different functional domains: MYB domain = DNA-binding domain, NLS = nuclear localization signal, NES = nuclear export signal, LZ = Leucine zipper (= assumed dimerization domain). Adapted from Wüstenhagen (2017) with modifications from Strunk (2023).

The amino acid sequence matches that of murine Mypop by more than 80% concordance, with identical NLSs, NES, and leucine zipper, and an almost identical MYB domain (Wüstenhagen, 2014). The first publication dedicated specifically to the human MYPOP characterizes it as antiviral protein and an interaction partner of L2 (Wüstenhagen *et al.*, 2018). MYPOP was found to effectively suppress the early gene expression of HPV types 16 and 18, acting as a restriction factor. A significant reduction of MYPOP protein levels were detected in various HPV-transformed cell lines. This was not the case for the corresponding mRNA, which suggested a post-transcriptional elimination. Subsequent analyses of overexpressed oncoproteins E6 and/or E7 showed that E7 significantly represses MYPOP protein amounts, suggesting MYPOP degradation by E7. Additionally, transfection experiments, which re-/overexpressed MYPOP, demonstrated reduction in cell counts in both HPV and non-virally transformed keratinocytes, implying tumor-suppressing properties. As this reduction in cell growth was not limited to HPV-transformed cells, MYPOP is thought to exhibit general tumor suppressive properties beyond its hypothesized opposing role to c-MYB with respect to HPV (Wüstenhagen *et al.*, 2018). Supporting this assumption of a protective role of MYPOP in human cells, the protein has recently also been described as binding partner of nuclear G-actin, which represses epithelial-mesenchymal transition (EMT) (Du *et al.*, 2023). In the study of Du and his colleagues, it has been shown that MYPOP suppresses cell survival and migration, thereby strengthening the hypothesis of MYPOP as a tumor suppressor. EMT is a process that allows an epithelial cell to transition into a cell type with invasive, migratory and anti-apoptotic properties, which is associated with the development of diseases like fibrosis and cancer (Kalluri and Neilson, 2003).

In other contexts, MYPOP is mentioned rather sporadically: It was found as possible candidate for interaction with chaperone HSP70 (Galazka *et al.*, 2014) and the histone variant H2A.Z (Pünzeler *et al.*, 2017). The protein was detected as being enriched in a genome-wide study associating genetic variations with maternal mitochondrial DNA copy number (Workalemahu *et al.*, 2017) and plays a role in an 8-gene model used as a marker for diagnosis and prognosis of epilepsy (Zhao *et al.*, 2023). In addition, MYPOP was discovered to be one of the main transcription factors responsible for gene expression that promotes insulin receptor endocytosis and therefore was proposed as a target to treat insulin resistance (Tim *et al.*, 2023).

In summary, this suggests a complex role of the transcription factor MYPOP, involved in many different contexts of human diseases, requiring further research. This thesis follows the strong interest in exploring MYPOP, its tumor-suppressor properties and the potential therapeutic effects of its re-expression in tumor cells.

2.3.2 **MYPOP antibodies (Abs)**

Since the recent discovery of MYPOP, there has been a scarcity of research tools available for its study. Wüstenhagen used in her work the only existing MYPOP antibody (Ab) ab94406 at that time (Wüstenhagen *et al.*, 2018). This is a polyclonal Ab from the company Abcam. While polyclonal Abs are easier to obtain than monoclonal ones, they permanently require the use of animals for production. Moreover, polyclonal Abs are a mixture of Abs with different antigen epitopes (Stills, 2021).

Monoclonal antibodies (mAbs), on the other hand, can be produced over a long term in cell culture and bind to one specific epitope, which is of great interest for diagnostics and research. Production of mAbs starts with immunization of animals, mostly mice, with the antigen. After the immune response, Ab-producing B cells are isolated from the animal and fused with continuously dividing myeloma cells (Köhler and Milstein, 1975). The resulting hybrid cells, known as hybridomas, are screened to identify those that produce Abs specific to the target antigen. Selected hybridomas are cloned to ensure a stable and uniform production of Abs. Finally, when validated, the cloned hybridomas can be cultured in large quantities to produce mAbs (Zhang, 2012).

Up to now, the amount of purchasable polyclonal MYPOP Abs has increased, involving other companies (FisherScientific, 2024; AviaSystemsBiology, 2024). However, no MYPOP mAb is still available, and this thesis aims to fill that gap.

2.4 **Vector-based gene therapy as cancer treatment approach**

As already indicated, treatment of cancers remains limited. Apart from surgery, approaches like radiation and chemotherapy are still the most applied methods. These therapies are effective, however, they also face hurdles like multi-drug resistance (Szakács *et al.*, 2006) and serious side effects (Mukherjee, 2010). Non-specific traditional approaches like chemotherapy target generally all dividing cells explaining the high number of adverse effects. This is why scientists developed new strategies like immunotherapy or targeted therapy, designed to be more selective, aiming to both increase specific effectiveness and minimize damage to normal cells (Schirrmacher, 2019).

Gene therapy is one of these new approaches, involving the introduction, modification, or correction of genetic material within cells to treat or prevent disease (Weichselbaum and Kufe, 1997). Since tumor suppressors are known to play important roles in cancer development, their encoding genes are potential tools in gene therapy against cancer (Amer, 2014).

Strategies for introducing the desired genetic material into target cells fall into two broad categories: direct transfer (transfection) and transfer through vectors (transduction).

Transfection is considered safer and easier to modify (Glover, Lipps and Jans, 2005), but lacks high transfection rates and is more difficult in *in vivo* application (Yamamoto *et al.*, 2009). Viral vectors achieve high transduction rates and reliable transport *in vivo* (Chen, Keiser and Davidson, 2018), but in some cases, side effects like induced immune response or cytotoxicity have been reported (Glover, Lipps and Jans, 2005).

Based on different types of viruses, there are a variety of viral vectors that are designed to only transport genetic material of interest and not cause the original associated disease (Chen, Keiser and Davidson, 2018). One of these vector systems was developed from HPV and used initially *in vitro* (Zhao *et al.*, 1998). In 2004, Buck et al. established a protocol for the efficient production of HPV pseudovirus (PsV), by which genetic material can be packed into the HPV capsid, consisting of the two capsid proteins L1 and L2 (Buck *et al.*, 2004). Since then, HPV PsV have been used successfully with high transduction rates both *in vitro* (Raff *et al.*, 2013) and *in vivo* (Çuburu *et al.*, 2012; Mitsunaga *et al.*, 2011). Furthermore, HPV-derived vectors have shown preferential binding to tumor cells (Kines *et al.*, 2016). This is why they are of particular interest for this project.

3 Materials

3.1 Laboratory equipment

Table 1: Laboratory equipment

Product type	Name	Manufacturer
Analytical balance	Mettler AE 100	Mettler-Toledo
Blotting chamber	TransBlot™ Cell	Bio-Rad Laboratories
Camera	AxioCam HrM-Kamera	Zeiss
Cell counting chamber	Neubauer Improved	Marienfeld Superior
Centrifuges	Biofuge pico	Heraeus
	Fresco 21	Heraeus
	Labofuge 400R	Heraeus
	Le-80R ultracentrifuge	Beckmann
	Sorvall® RC-5B	DuPont Instruments
Freezing container	Mr. Frosty™	Thermo Fisher Scientific
Gel electrophoresis chamber	-	Bethesda Research Laboratories Inc.
Heating block	Blockthermostat BT 1303	HLC BioTech
Incubator	Hera Cell 240	Thermo Fisher Scientific
Laboratory balances	BL 1500 D	Sartorius
	Kern 510-41	Kern
Magnet stirrer	IKAMAG REC-G	Janke & Kunkel
Microscopes	Axiovert 200M	Zeiss
	Wilovert S AFL	Hund Wetzlar
Microwave	Micromat	AEG
pH-meter	InoLab pH Level 2	WTW, Weilheim
Pipettes	ErgoOne Single Channel Pipets	STARLAB GmbH
	Pipetus®-akku	Hirschmann Laborgeräte

Power-supply (SDS-PAGE & Western Blot)	Standard-Powerpack P25	Biometra
Shakers	Certomat R	B. Braun
	Rocky	Heraeus
Sterile Flow	Nu-440-400E (Class II)	NuAire
Sonicator	Bioruptor® Plus	Diagenode
Vortexer	MS1 Minishaker	Janke & Kunkel
Water bath	W12D	Peter Huber Kältemaschinenbau

3.2 Consumables

Table 2: Films and membranes

Product type	Name	Manufacturer
Nitrocellulose membrane	Amersham Protran™ 0.45 µm NC	GE Healthcare
Whatman paper	-	GE Healthcare
X-ray films	Super RX-N	Valmex/FUJI
	Amersham Hyperfilm™ ECL	GE Healthcare

Cell culture flasks, cell culture plates, falcons and all other plastic consumables were purchased from Applied Biosystems, Biozym, Eppendorf, Greiner, Sarstedt or Thermo Fisher Scientific. Laboratory glass utensils were purchased from Schott.

3.3 Chemicals, kit systems and reagents

Table 3: Chemicals, kit systems and reagents

Product	Manufacturer
Acetic acid (99.9%)	Carl Roth
Acrylamid stock solution (30%)	Carl Roth
Ammonium persulfate (APS)	Carl Roth
Bovine serum albumin (BSA)	Carl Roth
Brij®58	Merck KGaA

Fluorescence Mounting Medium	Agilent
Hoechst 33342	Merck KGaA
Lipofectamine™ RNAiMAX	Thermo Fisher Scientific
Lipofectamine™ 2000	Thermo Fisher Scientific
OptiPrep stock solution (60%)	Merck KGaA
PageRuler™ Prestained Protein Ladder (10 -180 kDa)	Thermo Fisher Scientific
Paraformaldehyde	Merck KGaA
Phosphate Buffered Saline (PBS, 10x)	AppliChem
Polyethylenimin (PEI)	Merck KGaA
TEMED	Carl Roth
Triton X-100	Perkin Elmer
Tween® 20	Carl Roth
Western Lightning™ Plus-ECL	Perkin Elmer
X-ray film developer/replenisher solution	Merck KGaA
X-ray film fixer/replenisher solution	Merck KGaA

All non-listed standard chemicals were purchased from AppliChem, Carl Roth, Clontech Laboratories, GE Healthcare, Merck KGaA, PAN-Biotech, Roche, Serva or Thermo Fisher Scientific.

3.4 Buffers and solutions

Table 4: Buffers and solutions

Name	Composition
Crystal violet staining solution	0.5% crystal violet powder (w/v) in ddH_2O
PBS (1x)	10% (v/v) PBS (10x) in ddH_2O
PBS-T (1x)	PBS (1x), 0.1% (v/v) Tween 20
Ponceau S staining solution	0.1% (w/v) Ponceau S, 3% (v/v) trichloro acetic acid in ddH_2O

SDS-PAGE 10x running buffer	250 mM tris-HCl, pH 6.8 2 M (w/v) glycerol 1% (w/v) SDS
SDS-PAGE 5x Laemmli sample buffer	312,5 mM tris-HCl (pH 6,8) 10% SDS 30% glycerol 0.2% bromphenol blue 10% ß-mercaptoethanol
SDS-PAGE polyacrylamide separation gel (10%)	14.2 ml ddH_2O 11.7 ml acrylamide stock solution (30%) 8.8 ml SDS-PAGE solution buffer B 350 µl APS (10%) 17,5 µl TEMED
SDS-PAGE polyacrylamide stacking gel (5%)	8.8 ml ddH_2O 2.5 ml acrylamide stock solution (30%) 3.75 ml SDS-PAGE solution buffer C 150 µl APS (10%) 15 µl TEMED
SDS-PAGE solution buffer B	1.5 M tris-HCl, pH 8.8 0.4% (w/v) SDS
SDS-PAGE solution buffer C	0.5 M tris-HCl, pH 6.8 0.4% (w/v) SDS
Western blot transfer buffer (1x)	25 mM tris 192 mM glycine 20% (v/v) methanol

3.5 Plasmids

Table 5: Plasmids

Name	Resistance	Reference
pShell16L1/L2wt	Ampicillin	(Buck *et al.*, 2004)
p3xFLAG-CMV-10 MYPOP	Ampicillin	(Wüstenhagen, 2014)
p3xFLAG-CMV-10 MYPOP-C	Ampicillin	(Wüstenhagen, 2014)

The two MYPOP plasmids were produced during Wüstenhagen's master's thesis and encode for proteins represented in Figure 5. MYPOP-AD (activation domain) corresponds to MYPOP-wt without the DNA-binding MYB domain (DBD) and is also called MYPOP-C (C-terminal) or MYPOP-ΔDBD.

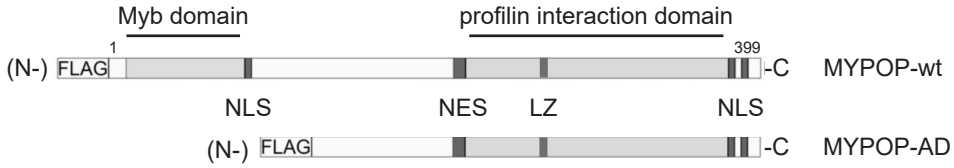

Figure 5: Schematic representation of FLAG-MYPOP-wt and FLAG-MYPOP-AD
The plasmid p3xFLAG-CMV-10 MYPOP encodes the protein MYPOP-wt and the plasmid p3xFLAG-CMV-10 MYPOP-C encodes the protein MYPOP-AD. MYPOP-AD equals the C-terminal part of MYPOP-wt without the DNA-binding MYB domain. Both proteins are FLAG-tagged. With kind permission adapted from Wüstenhagen (2017).

3.6 siRNA

Table 6: siRNA

Name	Sequence	Supplier/Reference
MYPOP #9	CGG CAT CGC CGC CAA GAT CAA	(Wüstenhagen, 2017), Merck KGaA
control-siRNA	AllStar Negative Control siRNA	Qiagen

MYPOP-specific siRNA was used for MYPOP knockdown (chapter 5.1.3). The AllStars Negative Control siRNA from Qiagen served as a negative control (Csi), comprising a sequence that does not correspond to any human genome mRNA nucleotide sequence.

3.7 Antibodies

The primary and secondary antibodies listed in Table 8 and Table 9 were used in the corresponding dilutions for Western blot (WB) and Immunofluorescence (IF) staining.

3.7.1 Primary antibodies

Table 7: Primary antibodies

Ab target	Specification	Species	Dilution	Supplier/ Reference
FLAG	M2	Mouse monoclonal	WB 1:10,000 IF 1:1,000	Merck KGaA
HPV16 L1	16L1312F	Mouse monoclonal	WB 1:300	(Knappe *et al.*, 2007)
MYPOP	Ab221487	Rabbit polyclonal	WB 1:1,000	Abcam
MYPOP	Ab94406	Rabbit polyclonal	WB 1:1,000	Abcam
β-actin	A5441	Mouse monoclonal	WB: 1:20,000	Merck KGaA
MYPOP	All numbered "# " Abs	Mouse monoclonal	WB: 1:1,000	DKFZ Heidelberg

3.7.2 Secondary antibodies

Table 8: Secondary antibodies

Name	Conjugate	Dilution	Supplier
Anti-mouse	Alexa Fluor 488	IF 1:450	Thermo Fisher Scientific
Anti-mouse	HRP	WB 1:10,000	Dianova
Anti-rabbit	HRP	WB 1:10,000	Dianova

All secondary Abs used in this work are polyclonal goat (species) Abs.

3.8 Cell culture

3.8.1 Cell lines

Table 9: Cell lines

Name	Description	Supplier or reference
HaCaT	Spontaneously immortalized human keratinocytes	CLS Cell Lines Service, Eppelheim
HEK 293TT	Derived from human embryonic kidney cell line 293, high expression of the large T-antigen from SV40	(Buck *et al.*, 2004)
Hela	Human cervix carcinoma cell line, HPV18 positive	DSMZ

NHEK	Primary normal human epidermal keratinocytes	PromoCell
Siha	Human cervix carcinoma cell line, HPV16 positive	(Friedl *et al.*, 1970)

Cell lines described in Table 10 were used for experiments in this work.

Additional follow-up experiments (5.4) were only evaluated as part of this project. Cell lines present only in the plates of the follow-up experiments are listed in Table 11. All lung tumor and primary lung cells (Table 11) were originally provided by M. Schneider, Thoracic Clinic of the University Hospital Heidelberg.

Table 10: Additional cell lines of the follow-up experiments

Name	Description
2106T	Derived from lung squamous cell carcinoma patients treated at Heidelberg University Hospital
2427T	Derived from lung squamous cell carcinoma patients treated at Heidelberg University Hospital
A549	Lung adenocarcinoma cell line with a KRAS G12S mutation
Primary lung cells	Derived from non-neoplastic lung tissue (at Heidelberg University Hospital)

3.8.2 Cell culture media and additives

Table 11: Cell culture media and additives

Name	Supplier
0.05% Trypsin-EDTA	Thermo Fisher Scientific
$CaCl_2$-solution	PromoCell
Ciprofloxacin (2mg/ml)	Fresenius Kabi
Cryo-SFM (freezing medium)	PromoCell
DetachKit (HEPES, 0.04% Trypsin-EDTA, Neutralization solution)	PromoCell
Dimethyl sulfoxide (DMSO)	Merck KGaA
Dulbecco's Modified Eagle Medium (DMEM) + GlutaMAX™	Thermo Fisher Scientific

Fetal calf serum (FCS, 10%)	Merck KGaA
HEPES-buffered saline solution	PromoCell
Hygromycin B (0.25%)	Carl Roth
Keratinocyte Growth Medium 2	PromoCell
Non-essential amino acids (100×)	GE Healthcare
SupplementMix	PromoCell

4 Methods

4.1 Cultivation of human adherent cells

All cell lines were maintained under sterile conditions as monolayers in T75 (75 cm²) or T175 (175 cm²) cell culture flasks. They were subcultured when reaching 80-90% confluency. Incubation was carried out at 37°C and 5% CO_2.

For experiments, cells were seeded in comparable quantities in 12-, 24-, or 48-well plates. To ensure comparable cell volumes, the Neubauer Improved cell counting chamber was used to determine the average number of cells per ml: Out of a cell suspension of 10 ml, 10 µl were pipetted into the chamber and the mean cell count of four squares was multiplied by 10,000 and the dilution factor.

4.1.1 Cultivation of immortalized and cancer cell lines

In this work, HeLa, HaCaT, HEK293TT, and Siha cells were cultured. They were cultivated in Dulbecco's Modified Eagle Medium (DMEM) supplemented with 10% FCS, 1% nonessential amino acids and 5 µg/ml Ciprofloxacin to avoid contaminations. HEK293TT cells were treated once per week with 200 µg/ml Hygromycin B to ensure T antigen expression.

For passaging, the medium was aspirated, cells were washed with PBS/EDTA (2.5 mM) and detached with 1 (T75) to 1.5 ml (T175) 0.05% Trypsin-EDTA. After an incubation time of 4 -10 minutes at 37°C and 5% CO_2, supplemented medium was added up to a final volume of 10 ml to inactivate trypsin. By pipetting up- and downward, remaining cells were detached and separated. Depending on cell density, 1/10 or 1/5 were transferred to a new cell culture flask and filled up to a final volume of 20 (T75) or 25 ml (T175) with fresh medium containing Ciprofloxacin. Remaining cells were used for experiments without the addition of antibiotics.

4.1.2 Cultivation of primary keratinocytes (NHEK)

Treatment of primary keratinocytes was carried out according to the manufacturer's protocol (PromoCell): NHEK were cultivated in supplemented Keratinocyte Growth Medium 2 (12.3 ml of SupplementMix and 0.6 µl $CaCl_2$ stock solution per 500 ml bottle of cell culture medium).

For passaging, NHEK were washed with HEPES-buffered saline solution and detached with up to 100µl 0.04% Trypsin/EDTA per cm² for 7-15 min at room temperature. Afterwards, the same amount of (trypsin) Neutralization solution was added, and the cell suspension was transferred to a 15ml centrifuge tube. Centrifugation at 300xg and room temperature was performed for 4 minutes. The supernatant was discarded, cells were carefully resuspended in 1 ml of the Keratinocytes Growth Medium 2 and depending on density, 1/10 or 1/5 were seeded

in new cell culture flasks containing prewarmed and supplemented Keratinocytes Growth Medium 2 (final volume T75: 20ml, T175: 25 ml). Cells remaining were used for experiments.

As this cell line is not immortal, it stops growing adequately after a certain time. Thus, to provide comparable conditions in experiments, these cells were only passaged six to eight times.

4.1.3 Cell stock storage

Long-term storage of the cell stock was carried out in liquid nitrogen. When preparing cell aliquots for cryopreservation, cells in confluent cell culture flasks were washed, detached, and neutralized in the same way as for passaging. After centrifugation of 300,000 cells (determined using the Neubauer Improved counting chamber) at 300 x g and room temperature for five minutes, the supernatant was discarded, and the cell pellet was resuspended in 1 ml 80% FCS/20% DMSO (immortalized and cancer cell lines) or 1 ml Cryo-SFM medium (NHEK) and transferred into a cryo vial. The vials were put into a freezing container (Mr. Frosty™) at -80°C for at least two hours, before transferring to a liquid nitrogen tank.

Thawing in order to cultivate the cells again took place in a water bath at 37°C for two minutes. Finally, after disinfection of the cryo vial with 70% ethanol, cells were directly placed into a cell culture flask containing the corresponding amount and type of supplemented cell culture medium and incubated.

4.2 Production of MYPOP-HPV16 pseudoviruses (MYPOP PsV)

HPV16 pseudoviruses (PsV) were established as a gene delivery tool as described earlier (Cerqueira *et al.*, 2017). To produce MYPOP-PsV or MYPOP-AD PsV for transduction of human cells with FLAG-MYPOP DNA, HPV16 PsV were generated according to a protocol of Buck et al. (Buck *et al.*, 2004). MYPOP-AD (see 3.5, Figure 5) was used to create a control virus due to the absence of a DNA-binding domain and the evidence that it does not affect the expression of HPV oncogenes (Wüstenhagen, 2017).

HEK293TT cells were seeded into T175 cell culture flasks and cultured in DMEM/10% FCS. At a confluency of 80 - 90%, cells from one T175 flask were divided among three new T175 flasks in 25 ml DMEM/10% FCS each. The following day, the HPV16 capsid expression vector (pShell16L1/L2wt) and either the MYPOP (p3xFLAG-CMV-10 MYPOP) or the MYPOP-AD (p3xFLAG-CMV-10 MYPOP-C) expression plasmid were introduced into the cells via PEI transfection: 25 µl pShell16L1/L2wt + 25 µl p3xFLAG-CMV-10 MYPOP or 25 µl pShell16L1/L2wt + 25 µl p3xFLAG-CMV-10 MYPOP-C were put together in 2.5 ml DMEM. After adding PEI/DEMEM (75 µl PEI in 2.5 ml DMEM) to each falcon, mixtures were incubated for 10 minutes at room temperature and applied to the corresponding cell culture flasks. Cells were then incubated at 37°C and 5% CO_2 to allow efficient transfection. Medium was changed

after five hours. After 48 additional hours of incubation for PsV production and maturation, cells were washed with PBS/EDTA (2.5 mM) and detached with 1.5 ml trypsin. Detached cells in DMEM were centrifuged in 50 ml falcons at room temperature and 200 x g for 10 minutes. Cells were washed with 20 ml PBS/$MgCl_2$ (9.5 mM) and again centrifuged for 10 minutes at room temperature and 200 x g. The obtained cell pellets were redissolved in 500 µl PBS/MgCl2 (9.5 mM) each and the resulting volume of approximately 700 µl was transferred to silicon-coated (low retention) Eppendorf tubes. Next, to achieve cell lysis and free DNA degradation, tubes were incubated for 24 hours with 35 µl Brij58 (0.5% end concentration) and 1 µl benzonase (0.1% end concentration) at 37°C and 5% CO_2. Vortexing was performed at regular intervals during incubation. Dilutions of the OptiPrep™ stock solution in PBS/NaCl (0.8 M), containing 39%, 33% or 27% (v/v) OptiPrep™, were prepared and stored at 4°C. The next day, density gradients for PsV concentration were prepared in ultracentrifuge tubes by sequentially adding 1.4 ml of each dilution starting at 39%. Gradients were stored for 1.5 hours at room temperature. The benzonase reaction in the silicon-coated tubes was stopped by adding 125 µl NaCl (5M). Cell lysates were placed on ice for 10 minutes and afterwards centrifuged at 2,000 x g and 4°C for 10 minutes to separate PsV from cell fragments. The supernatant, containing the PsV, was pipetted into the OptiPrep™ density gradients. They were centrifuged in a Le-80R ultracentrifuge at 234,000 x g and 16°C for 3.5 hours. The gradients were then divided into fractions by removing 300 µl at a time from the top and transferring to a new silicon-coated tube. Fractions were stored at 4°C.

To determine the fractions containing most of the FLAG-MYPOP plasmid-packed PsV (peak fractions), a transduction assay with HeLa cells was performed: 70,000 HeLa cells/well were seeded in a 24-well plate and 24 hours later, each well was infected with 5 µl of a different fraction. After another 24 hours of incubation, medium was removed, and cells were suspended in 5x Laemmli sample buffer. Finally, Western blotting was carried out using FLAG Ab and the determined peak fractions 9 - 12 (Figure 13) were pooled and used for experiments such as cell growth assays in this work.

4.3 Determination of cell number

To determine in vitro cell growth and survival, cell counts were determined. The method for cell number measurement in monolayer cultures according to Gillies (Gillies, Didier and Denton, 1986) was modified. Since light absorption of the unstained or destained cell layers is negligible, cell number measurements can be performed in the respective wells (Kueng, Silber and Eppenberger, 1989). Cells were seeded before a specific treatment and ultimately quantification of crystal violet staining was used in order to obtain statements concerning changes in cell numbers due to growth inhibition and/or cytotoxicity of the treatment.

In this work, determination of cell number was performed with different cell lines in 12-, 24- or 48-well plates. Cells were seeded and the treatment (MYPOP-wt PsV or purified protein MYPOP) or control treatment (MYPOP-AD PsV, OptiPrep solution or elution buffer of protein purification) was applied three times during an incubation period of 7 - 10 days. The concentrations of the treatments are given with the respective experiments.

For staining, cells were washed with PBS and fixed with ice-cold methanol (99.9%) for 10 minutes at room temperature. Methanol was discarded and crystal violet solution (0.5% crystal violet powder in ddH_2O) was added in a corresponding amount that covered the bottom of the wells. After one hour of incubation at room temperature, the crystal violet solution was removed, the plate was washed with water, and left to dry.

Stained plates were scanned with a quality of 1200 dpi and for quantification, colonies were analyzed using the plugin “colony area” of the program “ImageJ” (Guzmán *et al.*, 2014). The threshold used for analysis was adapted manually per plate based on a reference well to capture the growth pattern of each well as closely as possible. Figure 6 shows an example of successful threshold adjustment: The converted well after threshold adaptation (B) matches the growth pattern of the scanned plate (A). Results obtained by the subsequent measurement are given in Intensity [%], a percentage including both the covered area of a well and the color intensity after staining.

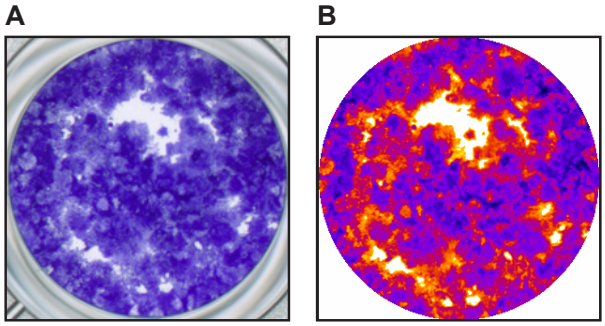

Figure 6: Threshold adaptation for determination of cell number
A Representative image of a well that is covered with HeLa cells after 2 weeks of incubation, stained with crystal violet. **B** Converted version of the same well after threshold adaptation, matching the pattern of cell growth in **A**

4.4 DNA and siRNA transfection

DNA transfection was used to introduce DNA into cells. Transfection reagents were PEI (see 4.2 for PsV preparation) and Lipofectamine 2000 (described below).

siRNA transfection is a laboratory technique used to introduce small interfering RNA (siRNA) into cells to silence specific gene expression through RNA interference. The molecules are short, double-stranded RNA sequences of about 17-25 nucleotides, designed to target a complementary mRNA sequence within the cell. Upon successful transfection, the siRNA is

incorporated into the RNA-induced silencing complex, which uses the siRNA strand to recognize and degrade the target mRNA, thereby preventing its translation into protein (Carthew and Sontheimer, 2009).

In this thesis, cell lysate of HeLa cells with MYPOP overexpression (transfected with FLAG-MYPOP expression plasmid and control siRNA = positive control) and MYPOP knockdown (transfected with FLAG-MYPOP expression plasmid and MYPOP mRNA-specific siRNA = negative control) was used for MYPOP-mAb validation (5.1.3). It was provided by other members of the Florin group according to the following protocol:

Comparable amounts of HeLa cells were seeded into 6-well plates. The following day, at a confluency of 90%, cells were transfected with FLAG-MYPOP expression plasmid (p3xFLAG-CMV-10 MYPOP) using lipofectamine 2000 as transfection reagent. Therefore, 4.0 µg DNA and 7.5 µl lipofectamine 2000 were separately added to each 250 µl DMEM. Both dilutions were mixed and incubated for five minutes at room temperature. Meanwhile, medium was exchanged for fresh medium (2.5 ml per well) and the mixture was subsequently added dropwise. The medium was replaced again after six hours in combination with siRNA transfection of either MYPOP-specific siRNA (MYPOP #9) or control siRNA (Qiagen) using lipofectamine RNAiMAX. Corresponding siRNA was diluted in DMEM to achieve a final working concentration of 20 µM. For each well, 2.25 µl of siRNA dilution and 4 µl of RNAiMAX were mixed separately with 250 µl RNase free DMEM. Both volumes were combined, gently mixed, and incubated at room temperature for 15 minutes to allow for complex formation. The transfection mixture with siRNA-RNAiMAX complexes was added dropwise to the cells. Afterwards, the cells were incubated at 37°C and 5% CO_2 for 48 hours. Finally, harvesting was performed using 325 µL of 2.5x Lämmli sample buffer containing 10% β-mercaptoethanol (Wüstenhagen, 2017; Strunk, 2023).

4.5 Sodium Dodecyl Sulfate Polyacrylamide Gel Electrophoresis

For separating protein samples based on their molecular weight, SDS-PAGE (Sodium Dodecyl Sulfate Gel Electrophoresis) was used in this work. It is a form of gel electrophoresis based on polyacrylamide. The proteins, due to the detergent SDS, are negatively charged, unfolding into linear chains and migrating to the positive pole in an electric field. They separate as smaller proteins pass through the polyacrylamide matrix more quickly.

Preparation of protein samples was carried out with 2.5x Laemmli sample buffer (5x Laemmli diluted 1:2), containing 10% ß-mercaptoethanol, followed by sonication (3 x 20 seconds on and off, set to high intensity and 4°C) to achieve complete cell lysis. Finally, samples were incubated at 95°C for 5 minutes. For 12-well plates, 70 µl of correspondingly diluted sample buffer were used per well. If samples were not used the same day, they were frozen at -20°C.

Gel production consisted of two different parts: First, the lower part, representing the separation gel with 10% polyacrylamide content, was produced. The composition of 14.2 ml ddH_2O, 11.7 ml acrylamide stock solution (30%) and 8.8 ml SDS-PAGE solution buffer B was mixed with 350 µl APS (10%) and 17.5 µl TEMED and poured into a chamber between two disinfected glass plates. A small amount of isopropanol (approximately 1 ml) was added and removed after 30 minutes. Then, the upper part, the stacking gel for sample concentration before entering the separation gel, was prepared. The ingredients were 8.8 ml ddH_2O, 2.5 ml acrylamide stock solution (30%) and 3.75 ml SDS-PAGE solution buffer C, mixed with 150 µl APS (10%) and 15 µl TEMED, and added on top of the solid separation gel in combination with a comb to shape the sample pockets.

After 30 minutes, polymerization was finished, and the gel was put into the gel electrophoresis chamber, filled with one liter of a 1:10 dilution (1x) of the SDS running buffer. At least one gel pocket was loaded with a marker (PageRuler™ Prestained Protein Ladder), and the other pockets with the prepared samples. Electrophoresis was performed at 200 V and 75 mA for 3 hours.

4.6 Western Blot (WB)

Western Blotting was used after SDS-PAGE to detect specific proteins in the samples. For this purpose, the protein pattern generated by protein separation was transferred from the gel onto a nitrocellulose membrane. First, the stacking gel was removed and the separation gel, containing the protein pattern, was placed on a nitrocellulose membrane. Two Whatman filter papers and a thin sponge were attached to each side, and altogether was soaked with WB transfer buffer and placed in a gel holder cassette. The cassette was inserted into a blotting chamber, which was subsequently filled with WB transfer buffer. An electric field of 400 mA was applied to the chamber perpendicular to the previous running direction of the proteins for two hours.

Successful protein transfer was checked by Ponceau S staining (Table 4), which shows all proteins non-specifically. The membrane was washed with PBS, and non-specific binding sites were blocked with PBS-T/5% skim milk for 20 minutes at room temperature. Then, primary Abs at the appropriate dilution (Table 6) in PBS/5% skim milk were added. Vessels containing the membranes and the diluted antibodies were placed on shaking devices and left for incubation at 4°C overnight. The following day, after washing three times with PBS-T, the secondary Ab (HRP-conjugated, Table 7), diluted 1:10,000 in PBS/5% skim milk, was added. Target of the secondary Ab is the species of the primary Ab. Incubation with the membrane took place on a shaking device for one hour at room temperature. After a washing sequence with PBS-T and PBS for 10 minutes and three times each, 1 ml of the two solutions of the

Western Lightning™ Plus-ECL kit was added. The HRP catalyzes luminol (the substrate included in the kit), which provokes temporary chemiluminescence. This signal was captured on X-ray films in a darkroom. When detecting β-actin as a loading control for comparable protein quantities in the samples, the same procedure of Ab incubation and signal acquisition on X-ray films was repeated afterwards with the primary Ab target β-actin.

4.7 Immunofluorescence microscopy

Indirect immunofluorescence (IF) microscopy was used to analyze expression and localization of MYPOP in cells after MYPOP-wt transduction and to estimate the transduction rate.

For this purpose, 30,000 HeLa cells per well were seeded on coverslips for microscopy in a 12-well plate. The following day, cells were infected with 2 µl MYPOP-wt PsV per well and incubated for 24 hours at 37°C and 5% CO_2. Next, cells were washed with PBS and fixed with 2% paraformaldehyde in PBS for 10 minutes and afterwards permeabilized with 0.2% TritonX-100/PBS buffer for 20 minutes at room temperature. After three washes with PBS within 10 minutes, blocking of non-specific Ab-binding sides was performed with PBS/1%BSA on a shaking device for 30 minutes at room temperature. The primary FLAG Ab was used to detect MYPOP via its FLAG-tag and diluted 1:1,000 in PBS/1%BSA. Next, 50 µl were applied onto each coverslip and left for one hour of incubation in a humid chamber at 37°C. Afterwards, the dilution was removed, and coverslips were again washed three times with PBS and blocked with PBS/1%BSA for 10 minutes on a shaking device at room temperature. The secondary, fluorophore-conjugated anti-mouse Ab Alexa Fluor 488 was diluted 1:450 in PBS/1%BSA, applied and incubated for 45 minutes in the same way as the primary antibody. Only the incubation was light-protected and 45 minutes instead of one hour. The Ab dilution was removed and a third incubation at the same conditions was performed for 15 minutes: 50 µl Hoechst 33324, diluted 1:10,000 in PBS/1%BSA were applied per coverslip for nucleus staining. At the end, cells were washed three times with PBS/1%BSA within 10 minutes and three times with PBS within 20 minutes on a shaking device. Using Fluorescence Mounting Medium, coverslips were attached to the microscope slides and left to dry overnight at 7°C.

Microscopy was performed at an Axiovert 200M microscope at 200x and 1000x magnification. Fluorescence images were taken using Axiovision deconvolution software (Carl Zeiss, Jena). To estimate transduction efficiency after PsV treatment, a ratio of total nuclei and cells with FLAG-MYPOP-wt fluorescence signal was determined based on 10 images at 200x magnification.

4.8 Statistics

Unless otherwise specified, all experiments were repeated at least three times as biological replicates. Using Microsoft® Excel for Mac (version 16.74), data of the intervention groups were normalized to the mean value of the respective control group or, in dilution experiments, to the mean value of the highest dilution. Standard deviation was determined, and further statistical analysis was performed with Graph pad Prism 9 software for Windows (version 9.4.1, GraphPad Software, San Diego, California USA): Presence of outliers was tested via ROUT method with Q set to 0.1%. No outliers were detected, otherwise they would have been removed from the data set. In all hypothesis testing scenarios, alpha was set to 0.05. Testing for normal distribution was carried out using Shapiro-Wilk test.

In normally distributed data sets, comparison between all groups was performed by Brown-Forsythe and Welch ANOVA test. Differences between two specific groups were analyzed by Dunnett's test.

In not-normally distributed data sets with, differences between all groups were measured by Kruskal-Wallis test. Differences between two specific groups were evaluated with Dunn's test.

Number of data points (“n”) per group and exact p-values for each statical test are given in the figure legend. Statistical significance of differences ($p \leq 0.05$) and not significant differences are additionally indicated in the graphs:

*	$p \leq 0.05$
**	$p \leq 0.01$
***	$p \leq 0.001$
ns	not significant

5 Results

5.1 Putative MYPOP antibodies as diagnostic tool

Based on the knowledge that normal human keratinocytes (NHEK) express endogenous MYPOP, while tumor cells either do not express it or show very low levels of expression (Wüstenhagen, 2014; patent16/206526, 2020), MYPOP level is of interest as a potential clinical marker. To be more precise, Abs that can differentiate between normal and tumor cells based on MYPOP, could be useful as additional tools in clinical practice, for instance in histochemistry.

Up to now, only polyclonal MYPOP Abs produced in rabbit are purchasable on the market. Thus, the Florin group, together with the collaborator from the Antibody Core Facility DKFZ (Heidelberg), produced monoclonal antibodies (mAbs) in mouse hybridoma cells to develop MYPOP Abs with higher production efficiency for research and diagnostic use. To test these mAbs, they were compared to the recognition patterns of the available polyclonal Abs in WB analysis of purified MYPOP protein and cell lysates from HPV18-transformed cells (HeLa), immortalized keratinocytes (HaCaT), as well as primary keratinocytes (NHEK).

5.1.1 Polyclonal antibodies detecting MYPOP differ in their signal patterns

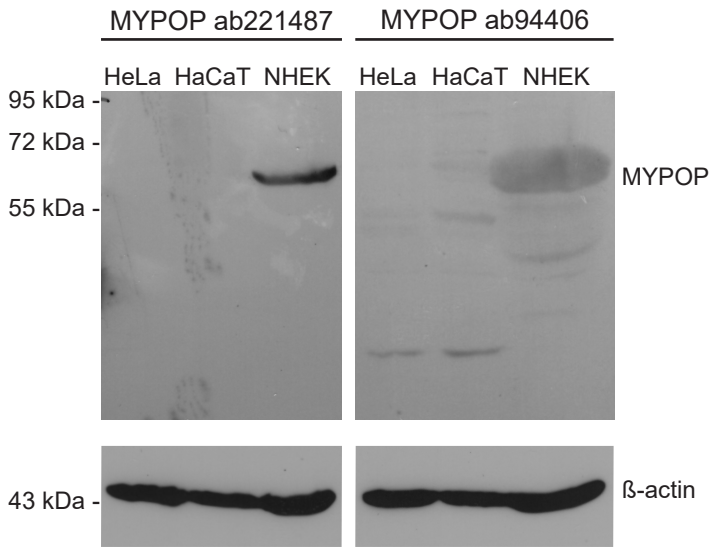

Figure 7: Polyclonal antibodies detect endogenous MYPOP expression in NHEK
WB comparing the endogenous expression of MYPOP in HeLa, HaCaT and NHEK lysates. MYPOP is detected at a WB run height of approximately 60 kDa with the polyclonal MYPOP Abs ab221487 and ab94406 from Abcam. β-actin (42 kDa) was used as a loading control.

The polyclonal MYPOP antibody ab94406 (Abcam) had been tested before and was considered useful to differentiate between normal and tumor cells (Wüstenhagen, 2017). At the time this thesis began, antibody ab221487 (Abcam) had just entered the market. To determine its detecting properties, an SDS-PAGE of HeLa, HaCaT and NHEK lysates, followed

by WB and detection with the two polyclonal Abs was carried out (Figure 7). As can be seen in Figure 7, both Abs detected a clearly visible and presumed MYPOP band at approximately 60 kDa in NHEK. In comparison to ab94406, which showed multiple (probably unspecific) bands in all three tested cell lines, it detected only one specific band. This property made it highly suitable for creating a very clear demarcation between normal and tumor cells and therefore it was subsequently (5.1.2) used as a positive control for the mAbs.

5.1.2 New MYPOP antibodies show large differences in specificity

The collaborator at DKFZ Heidelberg produced different mother- and subclones of MYPOP Abs in mice and preselected the promising ones for testing in WB. The clones are numbered, with the slashes separating the generations of cloning and the numbers indicating the respective subclone. First, an SDS-PAGE of purified MYPOP, followed by WB and detection with the two subclones #24/1 and #143/6 in comparison to ab221487 and ab94406 on MYPOP protein samples was carried out as a proof of principle (Figure 8).

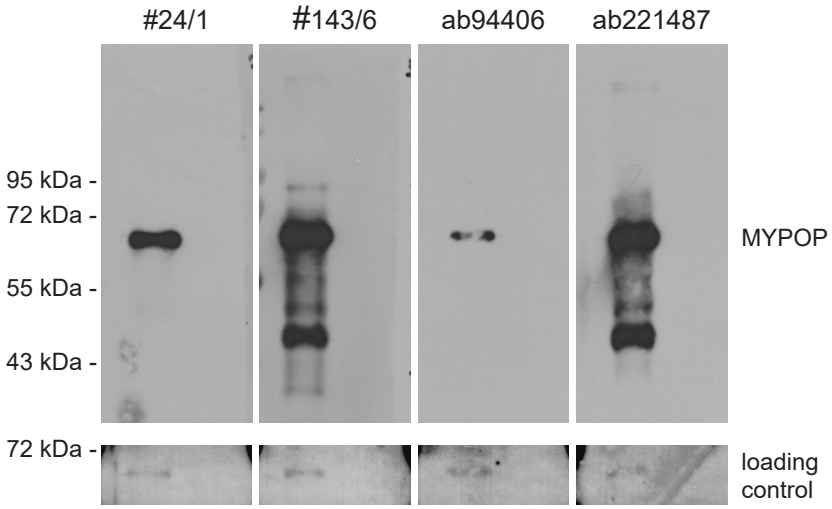

Figure 8: Monoclonal and polyclonal MYPOP antibodies detect purified MYPOP protein
WB analysis of purified MYPOP protein samples, comparing MYPOP detection of polyclonal rabbit Abs (ab94406 and ab221487 from Abcam) and subclones of mouse mAbs (#24/1 and #143/6). MYPOP protein had been purified by members of the Florin group in advance. For this experiment, 10µl per sample were mixed with the Laemmli preparation buffer. The monoclonal Abs were provided by DKFZ (Heidelberg). MYPOP was detected at its 60 kDa run height by all Abs. Additional bands at approx. 45 kDa were detected by #143/6 and ab221487. Ponceau staining of the MYPOP protein was used as a loading control.

The WB shows that both Abs #24/1 and #143/6 recognize purified MYPOP. Ab #24/1 detected one specific band at about 60 kDa, which is comparable to the pattern of ab94406. #143/6 showed a signal pattern like ab221487: both detected more than one band, with peaks at 60 and approximately 45 kDa.

For analysis of the different mother- and subclones, SDS-PAGE of HeLa, HaCaT and NHEK lysates, followed by WB and detection with the different mAbs in comparison to ab221487 was carried out (Figure 9).

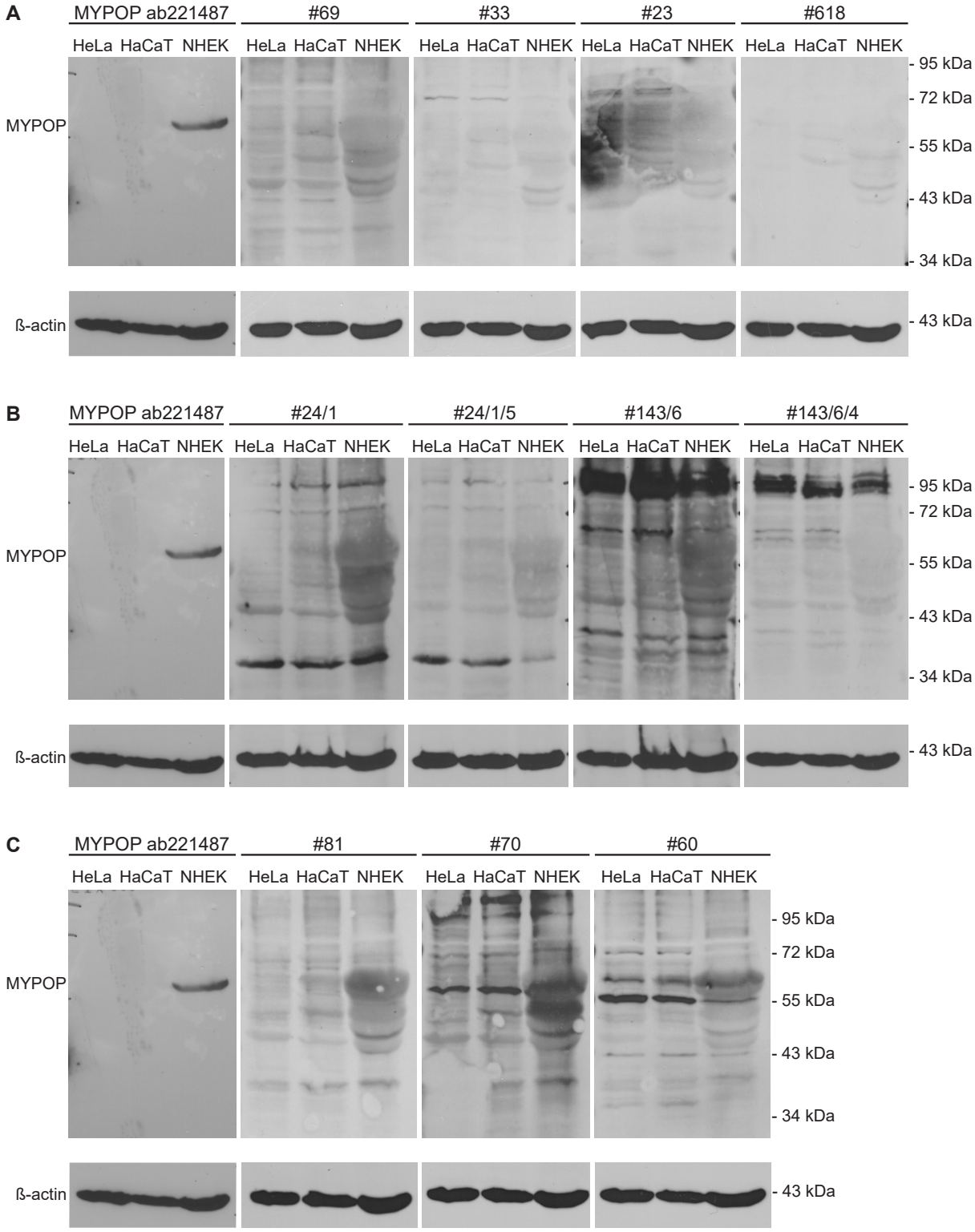

Figure 9: Detection pattern of monoclonal MYPOP Abs on HeLa, HaCaT and NHEK cells
WB analysis comparing signal patterns of preselected (DKFZ) MYPOP (m)Abs to the polyclonal MYPOP Ab ab221487 in HeLa, HaCaT and NHEK lysates. Mother- (**A** and **C**) and sub(sub)clones (**B**) of the (m)Abs were produced at DKFZ (Heidelberg). MYPOP shows a run height of 60 kDa in WB. β-actin (42 kDa) was used as a loading control.

Ab #69 (Figure 9, A) appeared to discriminate to some extent between normal (NHEK) and tumor (HeLa, HaCaT) cells, but several other bands were present as well. The clones #33 and

#23 (Figure 9, A) showed numerous unspecific bands. #618 (Figure 9, A) detected very little signal. Clones #24/1 and #143/6 showed the ability to distinguish (Figure 9, B), which is why further subcloning had already been performed by the collaborator. However, the subclones #24/1/5 and #143/6/4 (Figure 9, B) showed more background and less specific signal. The mother clones #81, #60, and #70 (Figure 9, C) showed the ability to distinguish between normal and tumor cells, with some non-specific bands. #81 appeared to be the best Ab here, detecting the main 60 kDa MYPOP band and weak unspecific signal. Because of this WB characteristics, #81 and #70 were chosen for further subcloning.

5.1.3 Identification of a suitable monoclonal MYPOP antibody

After successful subcloning (DKFZ), the mAbs were also tested in WB analysis. This time, the subclones were additionally tested on HeLa lysate with overexpressed MYPOP and MYPOP knockdown (provided by other members of the Florin group) as a second control in the WB analysis for validation (Uhlen *et al.*, 2016). The FLAG-MYPOP-expressing HeLa cells were either transfected with control siRNA (Csi) or MYPOP-specific siRNA (#9si) as described in 4.4. A representative WB selection of the second round of testing is shown in Figure 10.

All MYPOP-specific Abs recognized the overexpressed protein in HeLa. Unfortunately, subclones #81/19, #24/1/5, and #143/6/9 no longer recognized specific MYPOP bands in NHEK. They seemed to have lost reactivity.

In contrast, all subclones of #70/25 detected overexpressed MYPOP, lost their signal in MYPOP knockdown HeLa cells and were able to distinguish between tumor (HeLa) and normal (NHEK). The three mAb subclones with the most accurate signal (1, 4, and 5 of #70/25), are shown in the lower row of Figure 10. These MYPOP mAbs might be useful tools in research and in potential diagnostics for differentiating between normal and cancerous cells.

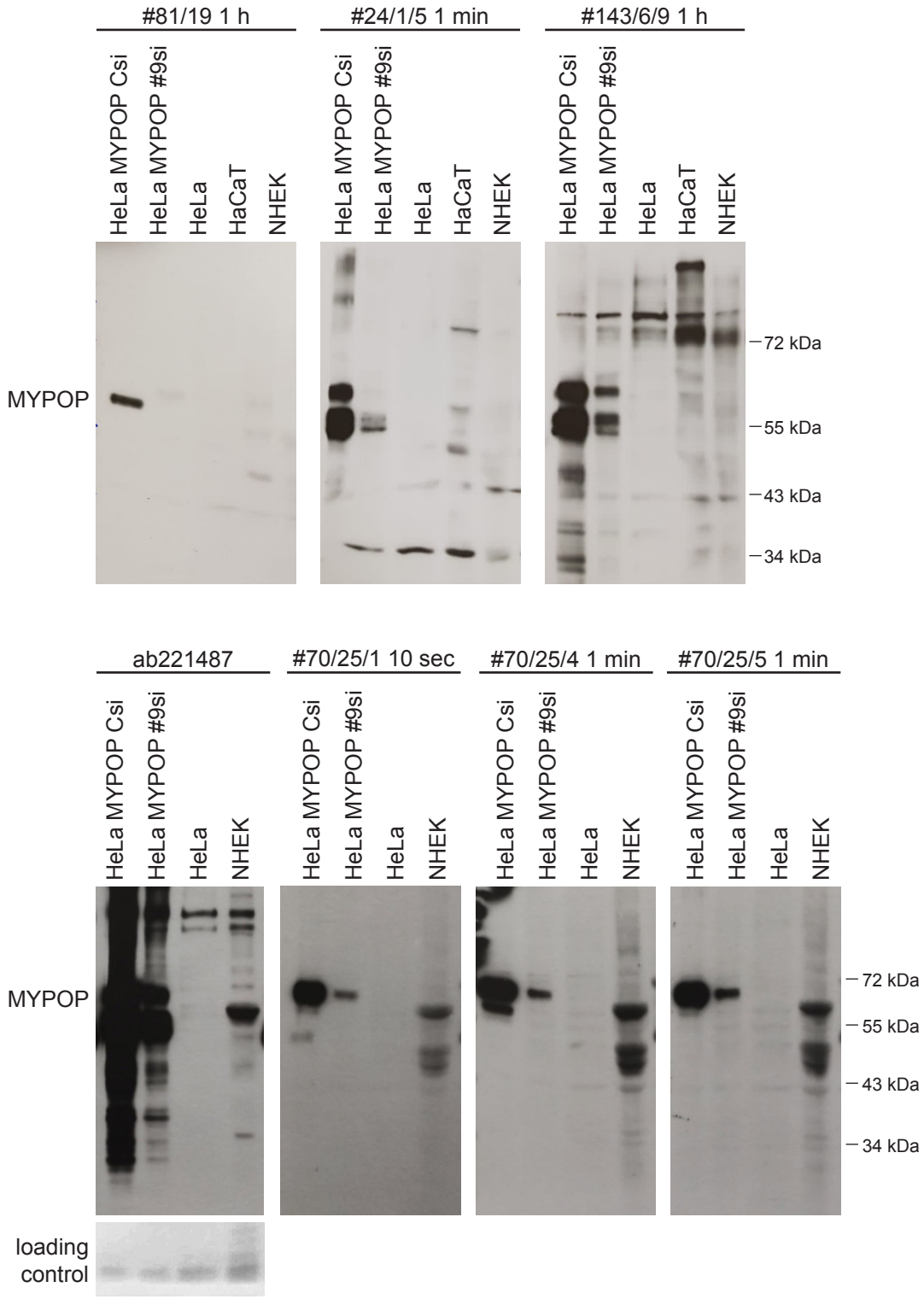

Figure 10: Further subcloned mAbs detect overexpressed and endogenous MYPOP in WB analysis
WB analysis comparing signal patterns of subcloned MYPOP mAbs to the polyclonal MYPOP Ab ab221487. The Abs produced by DKFZ (Heidelberg) were tested on lysates of NHEK, HaCaT, HeLa, HeLa treated with FLAG-MYPOP expression plasmid and transfected with control siRNA (MYPOP Csi = overexpression), HeLa treated with FLAG-MYPOP expression plasmid and MYPOP-specific siRNA (#9si = MYPOP knockdown). The Ab ab221487 (Abcam) served as a positive control for MYPOP-wt and the difference between HeLa (no detectable endogenous expression) and NHEK (well-detectable endogenous MYPOP expression). Out of motherclones #81, #24 and #143, only one subclone each is shown as representation of the lost reactivity with endogenous NHEK MYPOP protein. Of motherclone #70, the three best reacting subclones are represented in the lower row. Representative ponceau staining at 25 kDa is shown as a loading control.

5.2 Testing of MYPOP protein application to reduce cancer cell growth

Considering the tumor suppressive properties of MYPOP, it was of interest to analyze how MYPOP could find clinical application not only as a biomarker (5.1), but also as a potential drug to inhibit the growth of cancer cells. It was already known that transfection of the MYPOP expression plasmid reduces cell counts in colony formation assays of HPV-transformed cell lines (Siha, HeLa) and immortalized cells (HaCaT) (Wüstenhagen *et al.*, 2018). However, since these experiments had been performed with transfection reagents that are not applicable *in vivo*, other ways to apply MYPOP as a potential cancer therapy need to be explored.

Some proteins, like insulin, can be taken up by human cells by extracellular receptors without needing transfection or transduction mechanisms. Even though no specific MYPOP transporter is known, direct application of the protein on cancer cells was attempted first, as it had not been tested so far. Purified MYPOP, which had previously been produced by members of the Florin group, was used for this purpose. Since the protein was dissolved in elution buffer (according to Wüstenhagen, 2017 : 50 mM monosodium phosphate, 300 mM NaCl, 400 mM imidazole, pH 7.4), the first step was to clarify whether the imidazole-containing buffer showed cytotoxic side effects.

5.2.1 Elution buffer used for protein purification shows cytotoxic effect

HeLa and Siha cells were seeded into a 24-well plate and incubated for eight days with different dilutions (1:5,000 up to 1:10) of the elution buffer in cell culture medium to explore its effect. In order to quantify the cell growth, the determination of cell number was performed as described in 4.3. Intensity in % is a measure of the relative cell count, determined by the color intensity of the stain in combination with the area covered by cells in a well. In this experiment, the cell counts after treatment with dilution 1:5,000 were set to 100%.

The experiment was only repeated once because the cytotoxic effect, which causes a reduction in the color intensity of the crystal violet due to a reduction in the number of cells, was already very clearly visible to the eye (Figure 11, stained wells below the graphs). The plots in Figure 11 show the quantified, concentration-dependent cytotoxicity for both Hela (A) and Siha (B). Intensity was more reduced the less diluted the elution buffer: 44,04% (HeLa) and 91,2% (Siha) with 1:100 dilution, 13,84% (HeLa) and 15,58% (Siha) with 1:50 dilution, 3,85 % (HeLa) and 0,56% (Siha) with 1:10 dilution. The higher dilutions (1:5,000 and 1:500) did not appear to be significantly cytotoxic either in quantification (mean: 1:5,000 = 100%, 1:500 = 89,92% in HeLa and 101,86 in Siha) or in visual approximation. Thus, an experiment was subsequently performed applying purified protein within this dilution range.

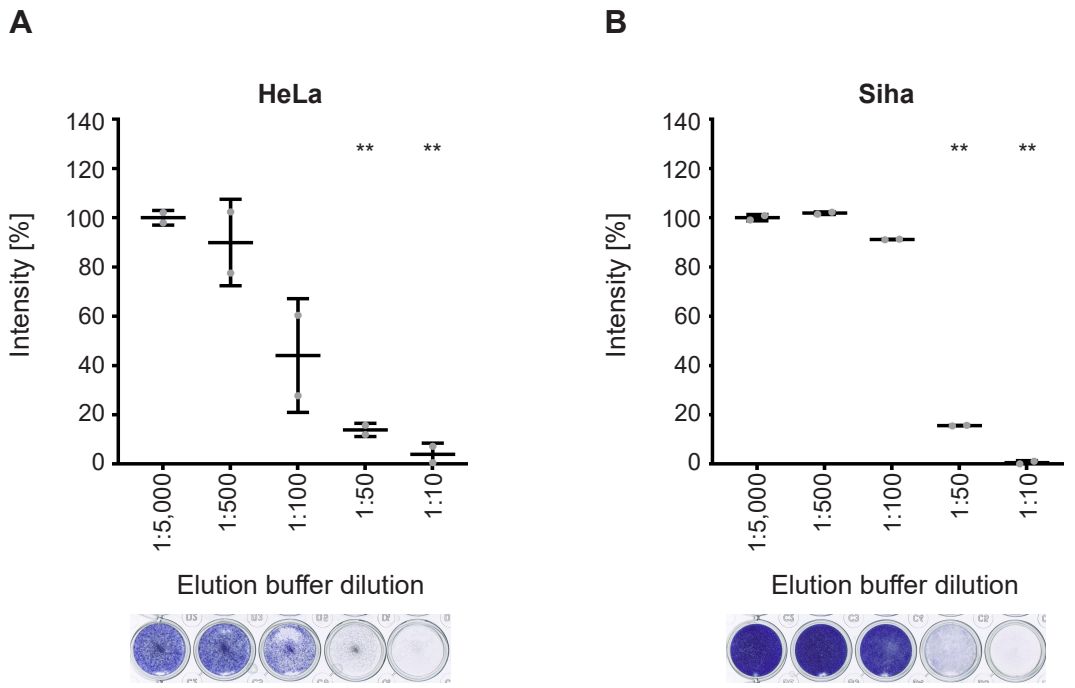

Figure 11: Elution buffer shows cytotoxic effect
HeLa (**A**) and Siha (**B**) were incubated for eight days with different dilutions of the elution buffer (used for MYPOP protein-purification) in cell culture media. Medium containing elution buffer dilution was exchanged every two to three days. The cells were fixed with methanol and stained with crystal violet. Representative wells are shown below the graphs. Colonies were quantified using “ColonyArea” plugin of the program “ImageJ”. “Intensity” combines covered area and staining intensity of a well. Reduced violet intensity indicates decreased cell counts. Highest dilution (1:5,000) was set to 100%. Out of two technical replicates (n = 2), significance was calculated using Kruskal-Wallis test and Dunn's test with: **A** p = 0.0095, p = ns for 1:50 vs. 1:5,000 and for 1:10 vs. 1:5,000, respectively. All p = ns for 1:100 vs. 1:5,000 and for 1:500 vs. 1:5,000, **B** p = 0.0011, p = ns for 1:50 vs. 1:5,000 and for 1:10 vs. 1:5,000, respectively. All p = ns for 1:100 vs. 1:5,000 and for 1:500 vs. 1:5,000. Values are presented as mean and SD.

5.2.2 Application of purified MYPOP indicates reduction of cell growth

Experiments with the determination of cell number were performed as described in 4.3. Here, HeLa cells were seeded into a 48-well plate and incubated for eight days with three different dilutions (1:5,000, 1:1,000 and 1:500) of the purified, in elution buffer dissolved, MYPOP protein in cell culture medium. In order to determine relative cell counts, the intensity after treatment with dilution 1:5,000 was set to 100%. After treatment with the 1:500 dilution, a significant reduction to 70% was detected (Figure 12). A slight, but not significant reduction to 94% after treatment with the 1:1,000 dilution can be observed as well. The effect can be seen in the diagram of the cell number quantification (A) and by eye (B). It appears to be concentration-dependent. However, it was clear from the previous experiment that the concentration could not be increased maintaining the same test settings. Earlier, during the purification process, Wüstenhagen had already tested transferring the protein into an imidazole-free solution, which led to precipitation of the MYPOP protein (Wüstenhagen, 2017). Non-soluble MYPOP protein is not applicable, which is why this approach was abandoned, and no repetition was performed.

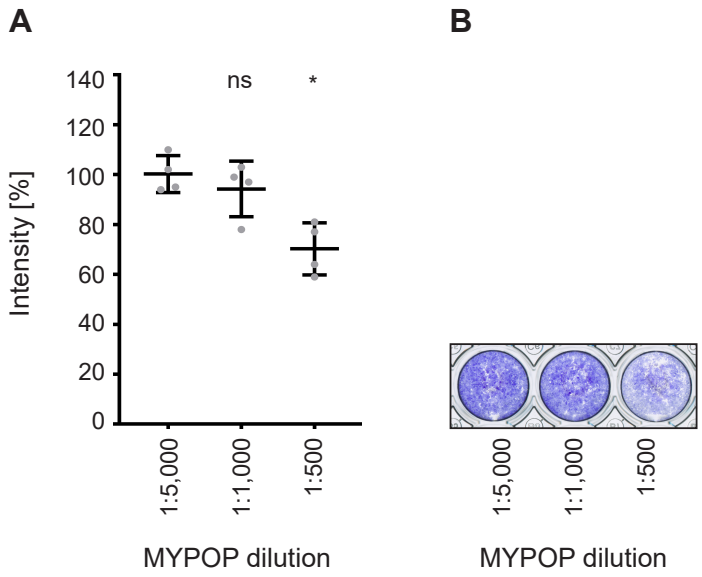

Figure 12: Purified MYPOP in elution buffer reduces cell counts in HeLa
Determination of cell number: HeLa were incubated for seven days in medium with different dilutions of the purified protein MYPOP (dissolved in elution buffer). Medium was exchanged every two to three days. The plate was fixed with methanol and stained with crystal violet. **B** shows representative cell stainings. Colonies were quantified using "ColonyArea" plugin of the program "ImageJ". "Intensity" includes covered area and color intensity of the measured wells. Reduced violet intensity indicates decreased cell counts. Highest dilution (1:5,000) was set to 100%. Out of four technical replicates (n = 4) from one biological replicate, significance was calculated using Brown-Forsythe ANOVA test, Welch's ANOVA test and Dunnett's test with p = 0.0054, p = 0.0131, p = 0.0143 for 1:500 vs. 1:5,000, respectively. All p = ns for 1:1000 vs. 1:5,000 and for 1:500 vs. 1:1,000. Values are presented as mean and SD in **A**.

5.3 Preparation of HPV16 pseudoviruses (PsV) as viral vectors

As an alternative approach to MYPOP transfection or direct application, transduction of the MYPOP-wt expression plasmid through viral vectors was tested. For this purpose, PsV constructed from HPV16 capsid containing either FLAG-MYPOP-wt or FLAG-MYPOP-AD (mutant without DNA-binding domain, see 3.5) expression plasmid were produced by transfecting HEK293TT cells according to the protocol of Buck et al. (Buck *et al.*, 2004, as described in 4.2). MYPOP-AD was used as a control for MYPOP-wt, because in former experiments it did not show any effect on the expression of oncogenes in HPV, suggesting its loss of function without the DNA-binding domain (Wüstenhagen, 2017).

In the last step of the production, a density gradient of Optiprep solutions containing the PsV was performed. The gradient was then fractionated from the top into fractions of 300 µl. As a control of the PsV production, 5 µl each were tested on HeLa. The cells were incubated for 24 hours, followed by WB analysis (Figure 13). FLAG Ab was used for detection. Both MYPOP-wt and MYPOP-AD levels could be detected in the typical PsV fractions 7 - 14. The peak fractions 9 - 12, showing the highest quantity (Figure 13), were pooled and used for transduction experiments described in the following subsections.

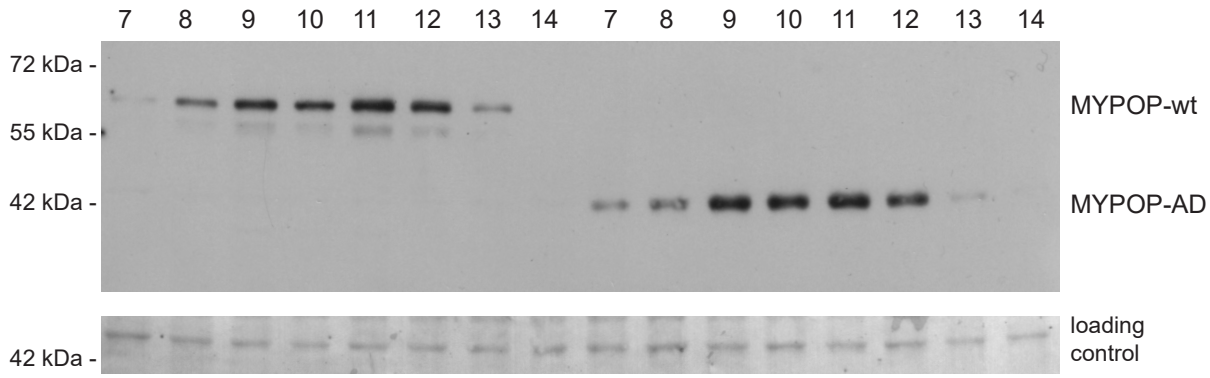

Figure 13: MYPOP detection in cells treated with peak fractions of the PsV gradients.
WB analysis comparing FLAG-MYPOP-wt and FLAG-MYPOP-AD levels in cells treated with different fractions (7 - 14) of the density gradient after PsV production. HPV16 PsV were produces as described in 4.2. The gradient was divided into fractions of 300 µl, and 5 µl of each fraction were applied on HeLa and incubated for 24 hours. SDS-PAGE followed by WB analysis was carried out and FLAG Ab was used for detecting both FLAG-MYPOP-wt (60 kDa) and FLAG-MYPOP-AD (40 kDa). Ponceau staining of the cell lysates at approx. 45 kDa was used as a loading control.

5.4 Analysis of MYPOP transduction

5.4.1 MYPOP-wt PsV reduces cell counts in HeLa

To analyze selective growth suppression by MYPOP transduction, experiments with tumor cells (HeLa, Siha) and normal cells (NHEK) were performed.

HeLa, Siha, and NHEK cells were seeded into 12-well plates and incubated for an average of eight days. Treatment with 2 µl of either 33% Optiprep (Opt.), MYPOP-AD PsV (M-AD) or MYPOP-wt PsV (M-wt) was carried out three times. Assays with determination of cell number were performed as described in 4.3. In order to determine relative cell counts, the intensity after Optiprep treatment was set to 100%. As can be seen in Figure 14, MYPOP-wt PsV treatment showed a significant reduction of cell growth in HeLa compared to Optiprep and MYPOP-AD PsV treatment (A). The mean of quantified intensity (including covered area and color intensity of the wells) after MYPOP-wt PsV treatment was 68.68%. In comparison to the control treatment Optiprep, this meant a reduction of 31.32%. In contrast, Siha (B) and NHEK (C) did not show differences in cell growth after both PsV treatments compared to the control. The Siha experiment was only repeated twice with the intention to save PsV from the same preparation for further analysis on HeLa, which showed a significant effect, and NHEK, as control for possible toxic effects on normal cells.

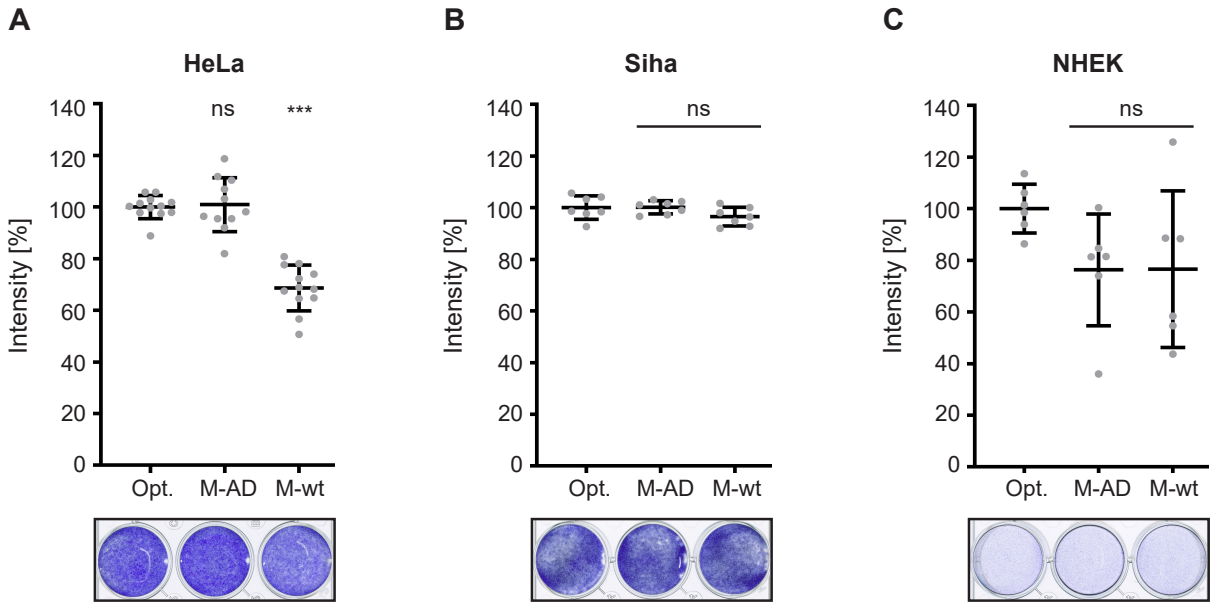

Figure 14: MYPOP-wt PsV reduces cell counts in HeLa
Determination of cell number: HeLa (**A**), Siha (**B**) and NHEK (**C**) were incubated for seven or eight days and treated three times at regular intervals with 2 µl of either 33% Optiprep solution (Opt.), MYPOP-AD PsV (M-AD) or MYPOP-wt PsV (M-wt). Plates were fixed with methanol and stained with crystal violet. Representative wells are shown below the plots. Colonies were quantified using "ColonyArea" plugin of the program "ImageJ". "Intensity" includes covered area and color intensity of the measured wells. Reduced violet intensity indicates decreased cell counts. Optiprep solution treatment (Opt.) was set to 100%. Values are presented as mean and SD. **A** n = 12 (11 for M-AD due to one contaminated well) from three biological replicates. Significance was calculated using Brown-Forsythe ANOVA test, Welch's ANOVA test and Dunnett's test with $p < 0.0001$, $p < 0.0001$, $p < 0.0001$ for M-wt vs. Opt. and M-wt vs. M-AD, respectively. All p = ns for M-AD vs. Opt. **B** n = 7 from two biological replicates. Significance was calculated using Brown-Forsythe ANOVA test, Welch's ANOVA test and Dunnett's test with all p = ns for M-wt vs. Opt., M-wt vs. M-AD and M-AD vs. Opt. **C** n = 6 from three biological replicates. Significance was calculated using Brown-Forsythe ANOVA test, Welch's ANOVA test and Dunnett's test with all p = ns for M-wt vs. Opt., M-wt vs. M-AD and M-AD vs. Opt.

5.4.2 MYPOP-wt PsV treatment shows concentration-dependent effect

To further characterize the growth inhibitory effect on HeLa, presented in Figure 14, Assays with determination of cell number using different volumes (dilutions) of the PsV preparations (0.125 µl – 4 µl) were performed as described in 4.3, with an incubation time of eight days. Different wells were treated three times with either 0.125, 0.25, 0.5, 1, 2 or 4 µl MYPOP-wt PsV at regular intervals of two to three days. Again, a reduction in cell counts was detected as can be seen in Figure 15. Compared to the cell growth of the 0.125 µl treatment (intensity = 100%), cells treated with 4 µl showed the biggest significant reduction in cell counts, with a mean of 67.93%. Reduction of cell number after 2 µl PsV treatment to a mean of 75.88% was also significant. By appearance of the stained wells, 1 µl of PsV preparation seemed to reduce cell growth. However, it was not confirmed statistically in this quantitative analysis. Overall, a concentration-dependent growth inhibitory effect of the MYPOP-wt PsV treatment on HPV-transformed cervical cancer cells was observed.

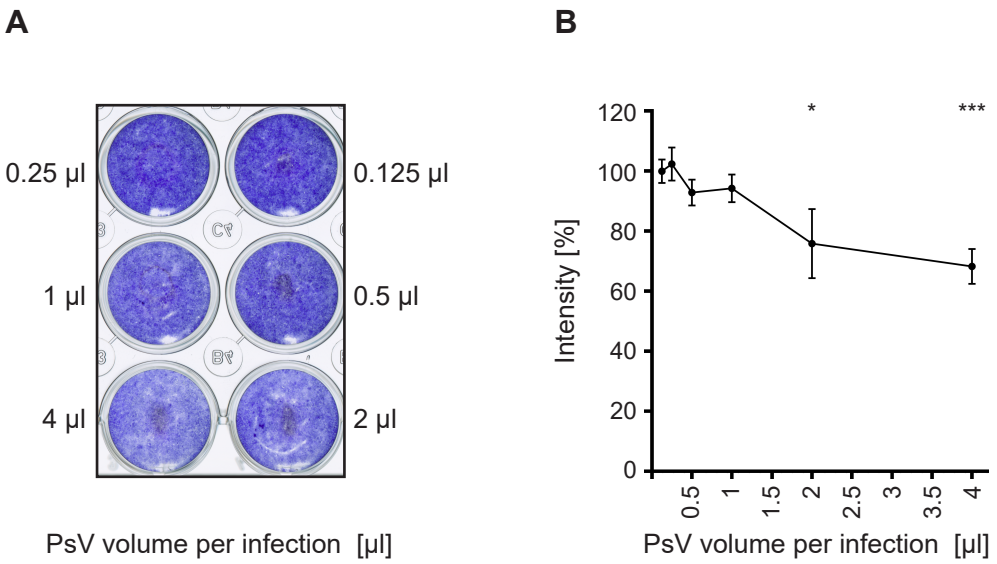

Figure 15: MYPOP-wt PsV shows a concentration-dependent growth inhibitory effect on HeLa cells. Determination of cell number: HeLa were incubated for seven days, and three times infected with different dilutions of MYPOP-wt PsV. Plates were fixed with methanol and stained with crystal violet. Representative cell stainings are presented in **A**. Colonies were quantified using "ColonyArea" plugin of the program "ImageJ". "Intensity" includes covered area and color intensity of the measured wells. Reduced violet color intensity indicates decreased cell counts. Highest dilution (0.125 µl) was set to 100%. Values are presented as mean and SD in **B**. n = 6 from two biological replicates (n = 4 for 0.25 µl, n = 3 for 1 µl due to a defective plate: Wells that were excluded from the analysis showed only 50% confluency). Significance was calculated using Brown-Forsythe ANOVA test, Welch's ANOVA test and Dunnett's test with $p < 0.0001$, $p < 0.0001$, $p = 0.0007$ for 4 µl vs. 0.125 µl, $p < 0.0001$, $p < 0.0001$, $p = 0.0280$ for 2 µl vs. 0.125 µl, $p < 0.0001$, $p < 0.0001$, $p = 0.0007$ for 4 µl vs. 0.25 µl, $p < 0.0001$, $p < 0.0001$, $p = 0.147$ for 2 µl vs. 0.25 µl, $p < 0.0001$, $p < 0.0001$, $p = 0.0017$ for 4 µl vs. 0.5 µl, $p < 0.0001$, $p < 0.0001$, $p = 0.0056$ for 4 µl vs. 1 µl, respectively. All p = ns for every other comparison.

5.4.3 MYPOP is detectable in HeLa and NHEK after transduction

The experiment described in 5.4.1 showed a reduction in cell growth in HeLa after MYPOP-wt PsV treatment, while cell counts in NHEK did not seem affected by the treatments. To further analyze this difference in cell growth behavior, the expression of both MYPOP-wt and MYPOP-AD in HeLa and NHEK after treatment was investigated. For this purpose, cells were treated as described in 5.4.1 and cell lysates were collected after 8 days. SDS-PAGE and WB analysis of whole-cell lysates were performed and stained for the FLAG epitope, allowing the detection of both FLAG-MYPOP-wt and FLAG-MYPOP-AD expression after PsV transduction. Figure 16 shows detectable FLAG constructs of MYPOP-wt and MYPOP-AD in both HeLa and NHEK after the corresponding treatment. The findings suggest that both HeLa and NHEK had been successfully transduced.

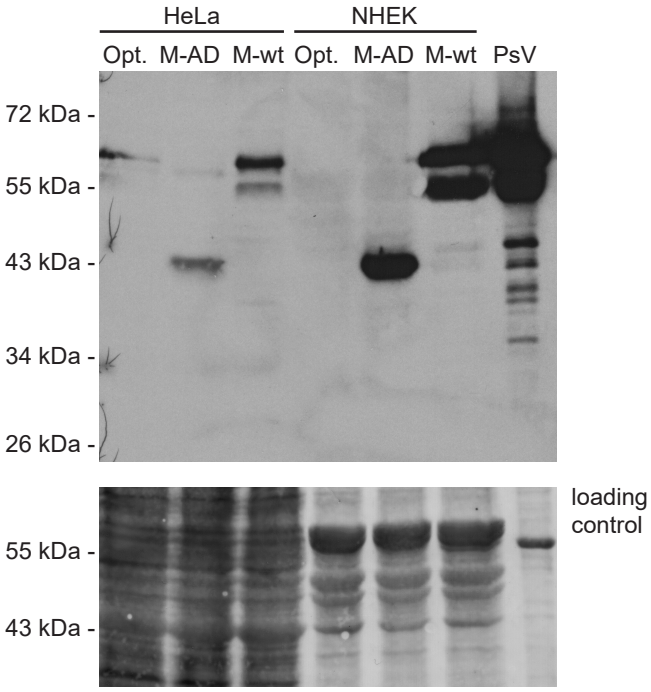

Figure 16: FLAG-MYPOP expression in HeLa and NHEK after transduction
WB analysis showing the expression of MYPOP in HeLa and NHEK lysates after PsV treatment: either MYPOP-AD PsV (M-AD), MYPOP-wt PsV (M-wt) or Optiprep solution 33% (Opt.) as a control were applied on HeLa and NHEK following the same protocol as described in 5.4.1. A sample of Laemmli only containing MYPOP-wt PsV is additionally shown to the right as reference. For MYPOP-wt and MYPOP-AD detection, FLAG Ab was used. MYPOP-wt can be detected at a run height of 60 kDa in WB, MYPOP-AD at a run height of approximately 43 kDa. Ponceau protein staining was used to compare amounts of cell lysate samples as a loading control.

5.4.4 **Transduction of MYPOP-wt PsV in HeLa cells is moderately efficient**

To further determine transduction efficiency in HeLa cells after PsV transduction, immunofluorescence (IF) assays were performed. Cells were treated with either MYPOP-wt PsV, MYPOP-AD PsV or 33% Optiprep. Twenty-four hours after transduction, IF staining and microscopy as described in 4.6 were performed. Based on ten images of approximately 16 cells per image, the transduction rate was estimated by counting cells with FLAG-specific fluorescence signal (green) in comparison to total nuclei (blue). This resulted in a transduction efficiency of about 44%.

Figure 17 shows parts of IF images at 200x magnification as representative examples. As expected, no FLAG signal was detected in HeLa after treatment with Optiprep (negative control, the lower row of Figure 17). Immunofluorescent signals after MYPOP-wt PsV infections are displayed in the upper row and indicate specific FLAG-MYPOP detection suggesting MYPOP expression in these cells. Staining of FLAG-MYPOP-AD is not shown, because no specific FLAG signal was detectable.

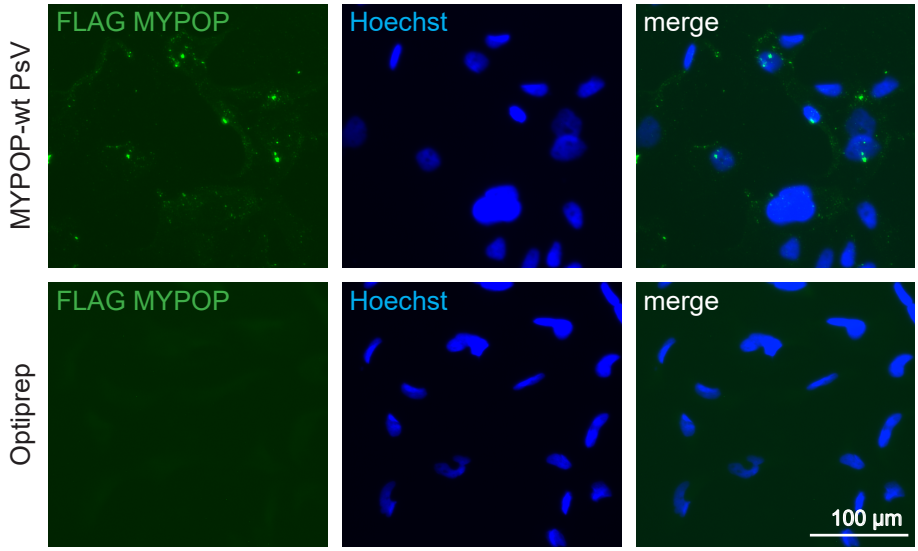

Figure 17: MYPOP-wt expression in HeLa cells after transduction
IF pictures of HeLa cells comparing detection of FLAG-MYPOP-wt (green) 24 hours post transduction via MYPOP-wt PsV (upper row of pictures) and control treatment with 33% Optiprep (lower row). FLAG-tagged MYPOP-wt was stained using FLAG Ab. Alexa Fluor 488 was used as secondary Ab. Hoechst 33342 was used for nucleus staining (blue). These images were taken at 200x magnification. Scale bar is shown in the right lower picture.

5.4.5 MYPOP-wt does not show a typical expression pattern post transduction

To obtain a more detailed view of the MYPOP localization, additional images at 1000x magnification were taken (Figure 18). To this end, the same IF staining experiment as in the previous section (5.4.4) was used.

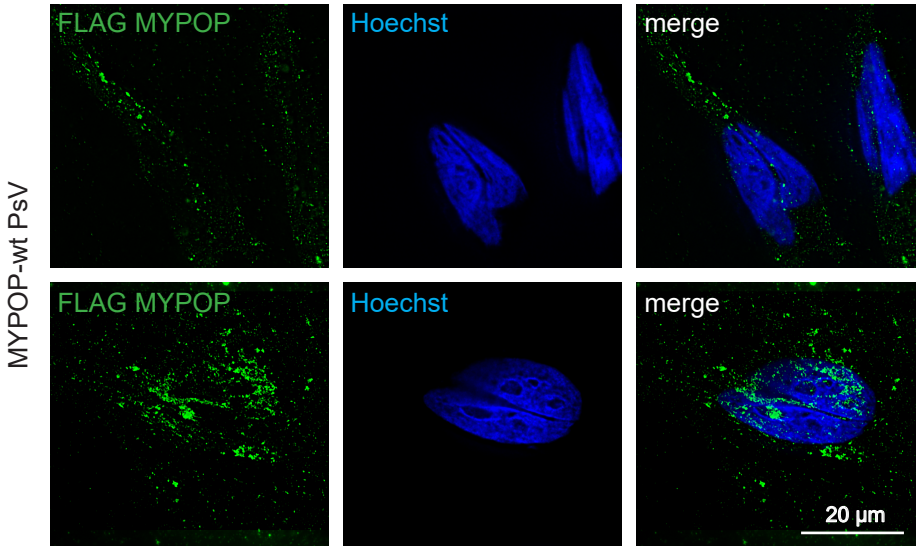

Figure 18: MYPOP-wt localization in HeLa after transduction
IF pictures of HeLa cells expressing FLAG-MYPOP-wt (green) 24 hours post transduction of MYPOP-wt PsV. FLAG-tagged MYPOP-wt was stained using the FLAG Ab. Alexa Fluor 488 was used as secondary Ab. Hoechst 33342 was used for nucleus staining (blue). These images were taken at 1000x magnification. Scale bar is shown in the right lower picture.

In contrast to earlier published MYPOP expression patterns showing nuclear localization (Lederer 2005, Wüstenhagen 2018), a punctate pattern of the fluorescent FLAG-tagged MYPOP signal was observed. The majority of the detected FLAG-MYPOP-wt punctate aggregates was observed in the cytoplasm of the cells.

5.4.6 **L1 is not detectable in MYPOP-AD PsV preparation**

As described in 5.4.5, no MYPOP-AD signal was detectable in the corresponding IF staining. To further characterize the MYPOP PsV, virus preparations were quantified by Strunk, a member of the Florin group. He used a Coomassie gel for L1 quantification. The MYPOP PsV concentration was about 1.5 µg in 25 µl, which corresponds to 0.06 µg/µl. Again, the viral L1 protein band was only visible in the MYPOP-wt PsV but not in the MYPOP-AD PsV preparation. This information led to the assumption that the MYPOP-AD PsV preparation lacked the important viral vector component L1.

To verify that hypothesis, the original membrane of the PsV preparation-treated cells, shown in 5.3 (Figure 13), was reused and stained with an L1 Ab (Figure 19).

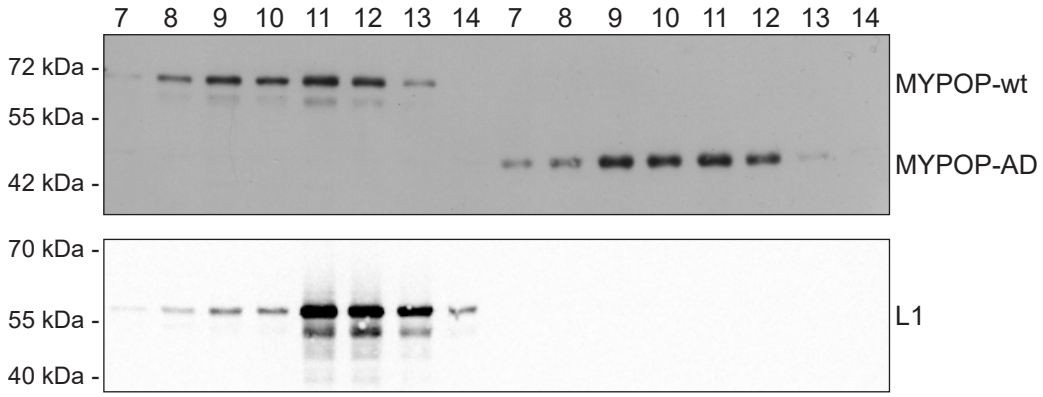

Figure 19: Missing L1 signal in MYPOP-AD preparation
WB analysis comparing L1 expression in FLAG-MYPOP-wt and FLAG-MYPOP-AD PsV preparation. The membrane of the transduction control experiment after PsV preparation (Figure 13) was reused and analyzed with L1 mAb. L1 levels can be detected in all fractions of the MYPOP-wt gradient (7-14 on the left), but not in cells treated with the MYPOP-AD PsV preparation (7-14 on the right).

This Western blot shows L1 detection in all cells treated with MYPOP-wt PsV fractions (Figure 19, left half of the Western blot), with a peak between fractions 11-13. In contrast, although the MYPOP deletion construct MYPOP-AD was present, none of the samples treated with MYPOP-AD PsV, showed the presence of the L1 protein (Figure 19, right half of the Western blot). This finding led to the following conclusion: First, the MYPOP-AD PsV production was not performed correctly as no L1 protein was present and therefore, no virus was produced. Second, the presence of MYPOP in the treated cell lysates was not a result of virus transduced and expressed MYPOP-DNA but rather indicated MYPOP presence in the PsV preparations which then attached to the treated cells.

5.5 Follow-up experiments with new PsV

To further test the effects of MYPOP PsV, later members of the Florin group performed new PsV preparations, including correctly prepared MYPOP-AD PsV as control virus. Additional controls were implemented such as a PsV preparation lacking an encapsulated plasmid. The presence of the L1 protein was immediately verified in all PsV preparations (not shown).

5.5.1 MYPOP-AD PsV treatment shows growth reducing effect in cervical cancer cell line HeLa

The growth-reducing effect of transduced MYPOP was analyzed by determination of cell number and compared with the findings of the initial experiments (5.4.1) of this project. Empty PsV (E) and a mock preparation (mock) were used as controls: Empty PsV were prepared by only using pShell16L1/L2wt plasmid without additional MYPOP expression plasmid in the virus preparation process. The mock control was prepared by using only FLAG plasmid in the preparation process without adding the packaging pShell16L1/L2wt plasmid. The effect of the new PsV compared to the controls (intensity after mock treatment = 100%) can be seen in Figure 20. A slight but not significant growth-reducing effect was observed for the MYPOP-wt PsV-treated cells (M-wt). A significant cell growth reduction was detected after MYPOP-AD PsV (M-AD) treatment: The intensity after MYPOP-AD PsV treatment was reduced to 75.05%.

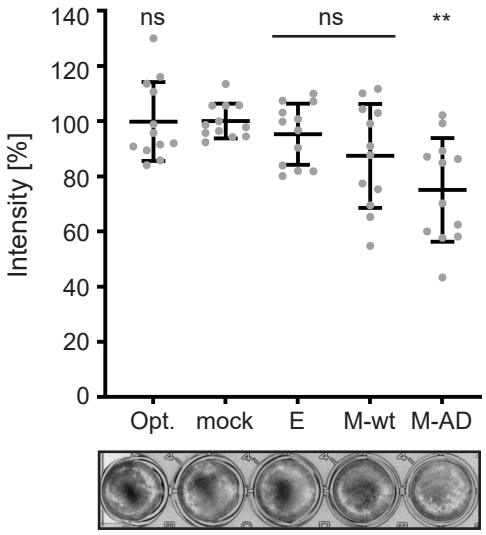

Figure 20: MYPOP-AD PsV treatment reduces cell growth in HeLa cells
Determination of cell number, stained plates kindly provided for analysis by the Florin group: 3,000 HeLa cells per well were incubated in 48-well plates for six days and treated four times at regular intervals with 1 µl of either 33% Optiprep solution (Opt.), FLAG mock preparation (mock) – produced according to the protocol of PsV preparation using FLAG plasmid without adding pShell16L1/L2wt, empty PsV (E) – PsV preparation using pShell16L1/L2wt without adding any plasmid, MYPOP-AD PsV (M-AD) or MYPOP-wt PsV (M-wt). Plates were fixed with methanol and stained with crystal violet. Representative wells are shown below the graph. For this thesis, the provided plates were analyzed: colonies were quantified using “ColonyArea” plugin of the program “ImageJ”. “Intensity” includes covered area and color intensity of the measured wells. Mock treatment (mock) was set to 100%. Values are presented as mean and SD. n = 12 from four biological replicates. Significance was calculated using Brown-Forsythe ANOVA test, Welch's ANOVA test and Dunnett's test with p = 0.0005, p = 0.0029, p = 0.0072 for M-AD vs. mock, p = 0.0005, p = 0.0029, p = 0.0148 for M-AD vs. Opt., p = 0.0005, p = 0.0029, p = 0.0445 for M-AD vs. E, respectively. All p = ns for every other comparison.

5.5.2 PsV show growth reducing effect in lung cancer cell line A549

To further analyze the tumor suppressive effect of MYPOP-PsV on lung cancer, PsV preparation was tested on lung cancer cell lines (2106T, 2427T, A549) and primary lung cells. Figure 21 shows the quantified effects on cell growth after treatment with either 33% Optiprep solution, Empty PsV, MYPOP-AD PsV or MYPOP-wt PsV. The intensity after Optiprep was set to 100%. No effect is seen on 2106T cell (A) and primary lung cell (D) growth behavior, while 2427T cells show a reduction of “Intensity” to 86.8% after empty PsV treatment (B). For A549 cells (C), a significant reduction after all three PsV treatments was detected with comparable growth inhibition of approximately 40% (means of crystal violet cell staining intensity: empty PsV 53.54%, MYPOP-AD PsV 60.75%, MYPOP-wt PsV 58.89%). These data suggest that treatment of A549 cells with the HPV16 capsid reduces cell growth of A549 independent of the encapsulated MYPOP DNA.

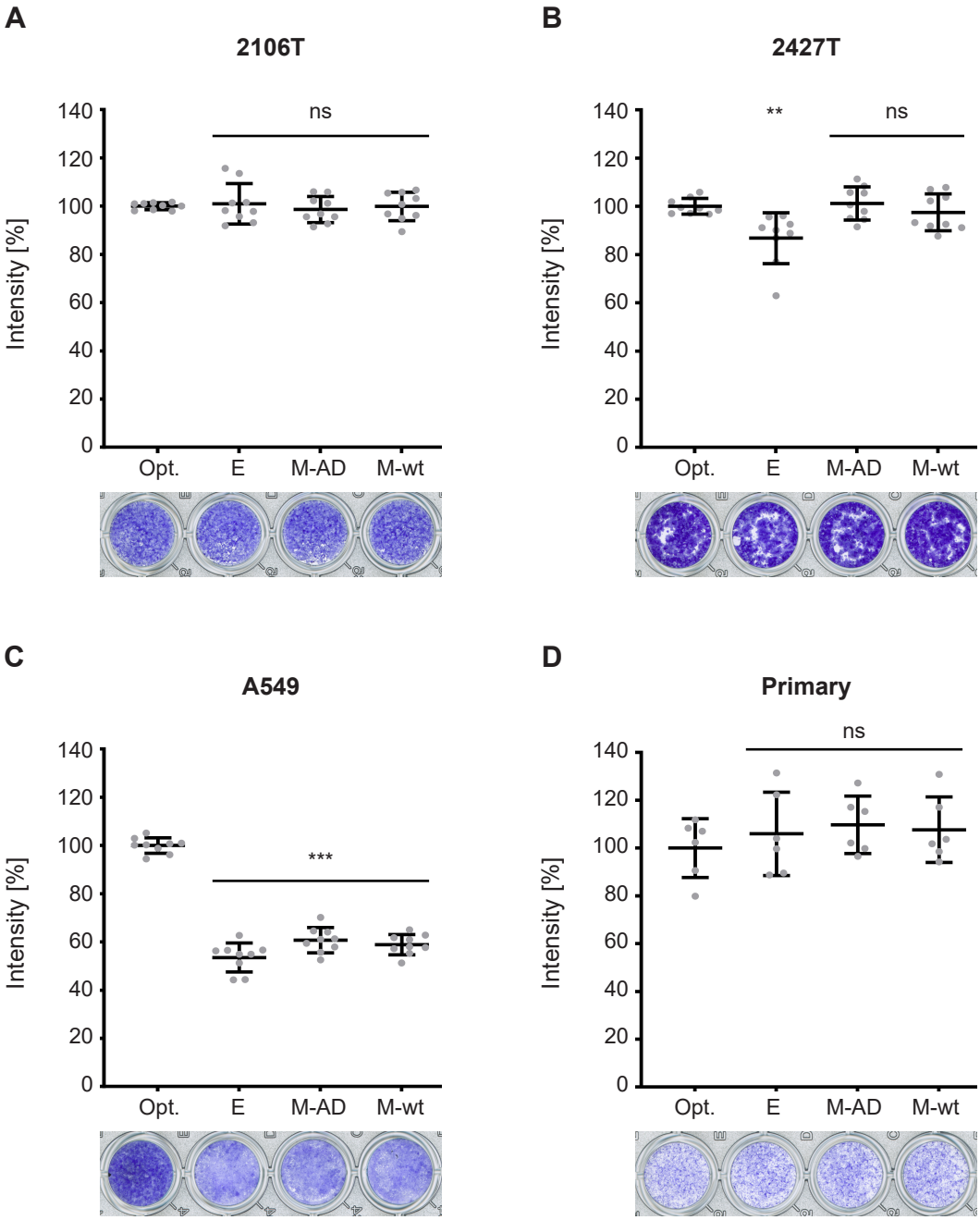

Figure 21: PsV treatment reduces cell growth in lung cancer cell line A549.
Assays with determination of cell number after different treatments of lung cancer cells 2106T (**A**), 2427T (**B**), A549 (**C**) and primary lung cells (**D**), kindly provided for analysis by J. Strunk. Cells were incubated for 10 days and treated three times at regular intervals with 0.5 µl of either 33% Optiprep solution (Opt.), empty HPV16 PsV (E), MYPOP-AD PsV (M-AD) or MYPOP-wt PsV (M-wt). Cells were fixed with methanol and stained with crystal violet. Representative staining is shown below the graphs. For this thesis, the provided plates were analyzed: colonies were quantified using "ColonyArea" plugin of the program "ImageJ". "Intensity" includes covered area and color intensity of the measured wells. Optiprep treatment (Opt.) was set to 100%. Values are presented as mean and SD. **A** n = 9 from three biological replicates. Significance was calculated using Brown-Forsythe ANOVA test, Welch's ANOVA test and Dunnett's test with p = ns for every comparison of means. **B** n = 9 from three biological replicates. Significance was calculated using Kruskal-Wallis test and Dunn's test with p = 0.0029, p = 0.0079 for E vs. Opt. and p = 0.0029, p = 0.0063 for E vs. M-AD, respectively. All p = ns for every other comparison of means. **C** n = 9 from three biological replicates. Significance was calculated using Brown-Forsythe ANOVA test, Welch's ANOVA test and Dunnett's test with p < 0.0001 in each test for M-wt vs. Opt., M-AD vs. Opt. and E vs. Opt. All p = ns for every other comparison of means. **D** n = 6 from two biological replicates. The third biological replicate was excluded due to no detectable growths of cells in any well. Significance was calculated using Brown-Forsythe ANOVA test, Welch's ANOVA test and Dunnett's test with all p = ns for every comparison of means.

6 Discussion

This work provides initial insights about the understudied tumor suppressor MYPOP and its possible applications in clinical practice in the context of cancer:

1) Diagnostic use: MYPOP is expressed in normal tissue, but undetectable in cervical and lung cancer tissue (Wüstenhagen *et al.*, 2018; patent16/206526, 2020), which implies potential clinical use as an additional biomarker for normal tissue in different applications such as immunohistochemistry. Polyclonal Abs have already been developed for use in research and are available commercially. In this work, new mAbs, produced in collaboration with the DKFZ Heidelberg, were characterized, and compared to the available polyclonal ones.

2) Therapeutic use: Following MYPOP's potential to reduce growth of tumor cells when overexpressed via transfection in cell culture (Wüstenhagen *et al.*, 2018; patent16/206526, 2020), two different application strategies were tested on normal and on tumor cells. On the one hand, the purified MYPOP protein was applied directly on cervical carcinoma cells. On the other hand, viral vectors (HPV16 PsV), containing the MYPOP expression plasmid, were produced and tested on different normal and tumor cell lines.

Overall, first, a monoclonal antibody (#70/25) detecting MYPOP specifically and reliably was identified. Thereby differentiating between normal and tumor cells, it was suggested for putative future diagnostic and research applications. Second, MYPOP application seemed to be able to selectively reduce cancer cell growth. In some tumor cell lines, a reduction in cell counts was detected after MYPOP protein or MYPOP-vector (PsV) application. In normal cell lines, none of the tested application types inhibited cell growth.

6.1 Methodological remarks

All experiments of this project were performed in cell culture (*in vitro*). The transferability of the results to possible effects/applications *in vivo* is limited but some helpful conclusions can be drawn. Possible *in vivo* applications can be speculated and would have to be investigated in future research. The cell lines used are a limited selection. Therefore, no general conclusions can be drawn for all tumor or normal cells.

In general, test power and sample size were not determined in advance because the experiments were intended to be initial and directional. Due to limitations in available funding and materials, such as purified protein, the ability to repeat all experiments was limited. When possible, three biological repetitions were performed. In case of deviations, the number of technical and biological replicates is precisely indicated. In such cases, a somewhat lower significance must be considered.

Both WB and IF analyses were not evaluated quantitatively due to the setting and objective of the experiments, which were of exploratory nature and aimed at protein detection rather than quantification.

6.2 Polyclonal antibodies detect multiple MYPOP forms

MYPOP is difficult to study because it is expressed at low levels and appears to exist in many different isoforms. The most prominent band is observed at 60 kDa, but there are also several higher and lower molecular weight forms (Wüstenhagen *et al.*, 2018). This complicates the analysis. An siRNA-mediated endogenous knockdown, which preceded the experiments of this work, was not possible (personal communication with L. Florin). This would have provided important insights into which bands are specific and which are not.

Through WB analysis, equivalence of the two polyclonal MYPOP Abs was shown. Both were able to detect MYPOP bands in NHEK lysate and in the purified MYPOP sample (see 5.1.1 and 5.1.2). Both polyclonal Abs detected a clear MYPOP band in NHEK and in the purified protein sample, which is consistent with the 60 kDa run height reported in the literature (Wüstenhagen *et al.*, 2018). Interestingly, ab94406 detected additional bands in NHEK lysate, whereas this was the case for ab221487 in the purified MYPOP protein sample suggesting unspecific detection of other cellular proteins or detection of different MYPOP forms by both polyclonal Abs. A possible Ab mix-up was checked several times and is very unlikely. In addition, the detection pattern of the already established Ab ab94406 applied on NHEK samples coincides with previously obtained assays performed by the Florin group (e.g. Wüstenhagen, 2017). The recognition pattern of ab221487 applied on purified MYPOP protein (Figure 8 - mainly two bands at about 45 and 60 kDa) is consistent with the results of Strunk, who repeated the purification in his thesis and used the same Ab for staining in WB (Strunk, 2023).

The reason for the distinct detection pattern of these Abs regarding purified protein and NHEK cells could be that different, post-translational modified (PTM = post-translational modification) forms of MYPOP are present in lysate vs. purified protein samples. The calculated weight of murine Mypop is 42 kDa, which should also be the case for the human orthologous protein due to its high similarity (Lederer, Jockusch and Rothkegel, 2005). In consequence, other bands might represent MYPOP (iso-) forms. The mobility shift of proteins in SDS-PAGE assays can occur through PTMs such as phosphorylation (Lee *et al.*, 2013). This is likely to be the reason for bands with different running behaviors in this case as well. The assumption is supported by a mass spectrometry and Lambda phosphatase treatment of purified MYPOP, performed afterwards by the Florin group. Both phosphorylation and acetylation sites of MYPOP were detected, and correlation between phosphorylation and molecular weight in WB

was confirmed (Strunk, 2023). Having a closer look at the exact amino acid sequences that the Abs detect, one can find ab221487 corresponding to aa 100 - 250 (Abcam, 2023) and ab94406 corresponding to aa 72 - 101 (product sheet of ab94406, kindly provided upon request by the manufacturer Abcam, see appendix) of MYPOP. The more N-terminal region (72 - 101) in contrast to 100 - 250, should be according to Strunk free of phosphorylation sites (Strunk, 2023) and thereby the Ab could detect differently phosphorylated isoforms of MYPOP. Accordingly, ab221487 is likely to recognize a specifically phosphorylated isoform with a WB running height of approximately 60 kDa, meaning that additional bands detected by this Ab could be degradation or cleavage products. Of course, it is similarly conceivable that the latter applies to bands of the other antibody (ab94406).

Yet, considering the WB analysis comparing normal and tumor cells (Figure 7), it is evident that both polyclonal Abs clearly mark the difference between normal and tumor cells based on MYPOP expression. The presence of additional bands, which are either unspecific or the result of MYPOP (de-) phosphorylation, degradation or cleavage processes, does not affect this function.

6.3 Good prospects for monoclonal MYPOP antibodies

In search of a MYPOP-specific mAb, promising candidates were selected according to their WB signals and were chosen for further development (5.1.2). Three subclones of Ab #70/25 were eventually identified and validated as markers for distinguishing between tumor and normal cells (5.1.3).

In the first testing round of Abs, most of the clones recognized the 60 kDa MYPOP band, but several additional bands as well. As mentioned in the previous chapter (6.1), the detection of different MYPOP forms is possible. This phenomenon can be seen in the purified protein detection (Figure 8): #24/1 recognized a band at about 60 kDa like ab94406, whereas #143/6 detected at least three other MYPOP bands at about 46, 50, and 56 kDa like ab221487. Nevertheless, it is currently assumed that MYPOP is almost absent in tumor cells (Wüstenhagen *et al.*, 2018) and therefore MYPOP forms should not be detectable in HaCaT or HeLa cells. Consequently, most other detected bands in the lysates seem to be unspecific. Non-specific binding of Abs has various causes and is mainly attributed to the recognition of additional targets, like endogenous Fc receptors (Buchwalow *et al.*, 2011). mAbs that do not bind to a MYPOP-specific epitope are useless for further research and were therefore not pursued.

In the subsequent testing of the further developed Abs (5.1.3), there was an unsuspected outcome: Although Ab #81 appeared to be the most specific Ab in the first WB analysis (Figure 9), it lost specificity for endogenous MYPOP in NHEK cells and recognized a weaker band of

overexpressed MYPOP after subcloning (Figure 10). This might be a specific PTM form that is absent in NHEK. While this is very interesting, it does not, however, render this Ab an appropriate marker.

In contrast, the subclones 1, 4, and 5 of #70/25 gained specificity and reactivity. They showed little to no signal in HeLa and comprised three well-contrasted bands at about 45, 48 and 60 kDa in NHEK. This suggests the binding of these subclones to specific PTM forms or putative isoforms of MYPOP. Genetic validation (according to Uhlen *et al.*, 2016) of the subclones by recognition of overexpressed MYPOP in HeLa and decreased signal after knockdown was also possible (Figure 10). Overall, the specificity seems on par with or better than that of the polyclonal Abs, differentiating very clearly between tumor (HeLa) and normal (NHEK) cells. So far, the goal of finding a precise mAb was achieved. This assumption is supported by the subsequent work of Plath, who again validated the #70/25 subclones in WB analysis of HaCaT cells, and performed IF assays with different subclones. In his conclusion, the same three subclones were found to work reliably in WB and #70/25/5 also in IF. In addition, the binding epitope of #70/25/5 was determined to be the MYPOP-AD (Plath, 2021). Further tests of these MYPOP mAbs in immunohistochemistry and ELISA (unpublished data of the Florin group) also showed precise antigen detection.

Nevertheless, it has not yet been clarified in which cases MYPOP levels are a reliable criterion to distinguish between normal and tumor tissue. A first step addressing that question was made by testing human lung tumor tissue, detecting differences between lung tumor and normal lung cells based on MYPOP isoforms (Strunk, 2023). To follow up on this matter, large-scale studies would have to be performed on many tumor types to determine MYPOP levels. Finally, it would also be of great interest to investigate MYPOP suppression, possibly acting as a driver mechanism in tumors (Tomasetti *et al.*, 2015).

6.4 Evaluating the inhibitory effect of purified MYPOP application on cell growth

To test the therapeutic potential of MYPOP, the purified protein was examined in direct application. It was found that the elution buffer, in which MYPOP protein was dissolved, had a significant concentration-dependent toxic effect (5.2.1). Nevertheless, in the subsequent application of the dissolved MYPOP protein in small concentrations, an inhibitory effect on cell growth was observed (5.2.2).

The elution buffer experiment (Figure 11) should be regarded as a mere point of reference in statistical interpretation, given the limited number of replicates. Nevertheless, the two technical replicates clearly identified the very attenuated cell growth (survival and or proliferation) after

incubation with the highest concentrations (1:50 and 1:10). The reason for this cytotoxic effect can be discussed based on the ingredients of the buffer. For high phosphate, there has been described a pro-apoptotic effect in HeLa and HEK cells (He *et al.*, 2020). Nevertheless, this effect was only seen with extracellular amounts of 40 mM. In the experiment of this work, the contained 50 mM monosodium phosphate was diluted at least 1:10, resulting in smaller phosphate concentrations. At lower phosphate concentrations, even promotion of cell proliferation was observed in the above-mentioned study. Regarding imidazole, at least for imidazole ionic liquid, there has been shown a versatile cytotoxic effect on HeLa cells already at small concentrations like 0.2 µg/mL (Xia *et al.*, 2018). This is still a higher concentration than used in this work, but a cytotoxic effect causing the observed cell death even at lower concentrations cannot be ruled out.

The dialysis process in order to remove the elution buffer was found to precipitate the MYPOP protein, rendering this approach unsuitable (Wüstenhagen, 2017).

In the second experiment of this section, in which the purified protein (dissolved) was applied to HeLa (5.2.2), cell reduction was observed upon the dilution of 1:500. The sole application of elution buffer in the same concentration did not show a significant reduction in cell growth (Figure 11). Thus, the possibility exists that the observed effect is caused by MYPOP. Nevertheless, the experiment was performed only once with four technical replicates due to low supplies of purified protein. Considering that and the unresolved question of at which concentration exactly the elution buffer alone already acts cytotoxically, the effect cannot be clearly attributed to MYPOP. Another argument against an effect of external MYPOP application is that so far only intracellular functions of MYPOP are known (see chapter 2.3). For MYPOP, being a TF, it would be unusual to have corresponding receptors or uptake mechanisms in cells. To investigate the observed unclear result further, it would be necessary to transfer the MYPOP protein into a suitable buffer. But taken together, other application types, as discussed in the following section, seem more promising so far.

6.5 Evaluation of PsV preparation and MYPOP transduction

HPV16 PsV were produced for transferring the MYPOP expression plasmid (MYPOP transduction) and tested on different cell types. The performed experiments (5.4.1 and 5.4.2) suggested an inhibiting, concentration-dependent effect of MYPOP-wt transduction on cell growth in HPV18-transformed HeLa cells compared to no effect in HPV16-transformed Siha cells and normal NHEK. In later experiments and further analysis of the transduction (5.4.4 – 5.4.6), an error in the control virus preparation was noticed. This implies a limited possibility to interpret the corresponding results. Therefore, in chapter 5.5, follow-up experiments with correct control PsV preparations were additionally evaluated as part of this project. In those

experiments, an effect of PsV preparations on cell number was detected for MYPOP-AD PsV in HeLa, and for all PsV preparations, including empty HPV capsids, in one type of lung tumor cells (A549).

6.5.1 Defective MYPOP-AD PsV preparation

In this thesis, MYPOP transduction was attempted for the first time (5.3), and therefore, HPV PsV were produced as vectors. Buck's protocol for the PsV preparation was known and established in the Florin group (see 4.2), but the MYPOP expression plasmid had never been packaged before.

Following the production of the new MYPOP PsV, testing with HeLa cells demonstrated that MYPOP-wt and MYPOP-AD expression peaks were present in cells treated with fractions 9 - 12 (Figure 13). Therefore, it was assumed that both MYPOP-wt and MYPOP-AD expression plasmid had been successfully packaged into the capsid and transduced into the cells. From previous PsV productions, it was known, that the PsV accumulate between fractions 7 to 14, which is why these fractions were tested. This is in line with the results of a subsequent analysis of the MYPOP PsV production conducted by Strunk, who identified the peaks for the capsid proteins L1 and L2 between fractions 10 and 13 in a comparable preparation (Strunk, 2023).

However, it was later found that neither the quantification of MYPOP-AD PsV nor L1 detection in the corresponding peak fractions was feasible (5.4.6). Subsequently, an effort was made to elucidate the reasons behind the failure of the MYPOP-AD PsV preparation, in contrast to the success of the MYPOP-wt PsV preparation. Unfortunately, it cannot be completely traced why there is no capsid protein detectable in the MYPOP-AD preparation and therefore probably no PsV at all. A possible explanation would be that L1 and L2 expression plasmids were not transfected into the PsV producing HEK cells. Either due to a faulty transfection or an error in the execution of Buck's protocol. It is striking that with sole MYPOP expression plasmid addition in the production process, the protein should only be detectable up to fraction 9. MYPOP enters the higher fractions of the Optiprep gradient only through an interaction with L1 or L2 (Strunk, 2023). Another confusing observation is the MYPOP-AD (FLAG) detection in WB (Figure 16), which was absent in IF (5.4.4). It would be reasonable to posit that, even if the MYPOP-AD in the WB only adhered to the cells, it should have been detectable in the IF in a similar manner.

Although the error and its related outcomes in WB and IF cannot be adequately explained, it can be summarized that the application of the MYPOP-AD “PsV” preparation of chapter 5.3 was in fact an Optiprep solution containing pure FLAG-MYPOP-AD. Its application should be

interpreted with extreme caution and cannot be used as an adequate control when interpreting the effect of MYPOP-wt PsV.

6.5.2 Pseudoviral effect in HeLa and lung cancer cells

The first transduction experiment (5.4.1) showed an inhibiting effect of MYPOP-wt PsV on cell growth in HeLa cells. Compared to the Optiprep solution, it provoked a reduction of almost a third. Due to the defective MYPOP-AD control “virus” (see previous chapter 6.5.1), this effect can be described in comparison to the Optiprep control but cannot be attributed clearly to MYPOP-wt. The comparable follow-up experiment on HeLa cells supports doubts about attributing the effect to MYPOP, as it showed a significant reduction only for PsV containing the MYPOP-AD construct. Both experiments have in common, that some PsV preparations showed quite clear cell growth-inhibiting effects. In addition, due to the experiment in chapter 5.4.2, it can be assumed that this effect is concentration-dependent.

The follow-up experiment on HeLa cells (5.5.1) was performed with two different PsV preparations and two different batches of plates to obtain four biological replicates. When analyzing the cell growth in the plates, it stood out that one of the plates showed a blurred growth pattern after staining. Excluding this plate, the results of the other ones also showed a significant cell growth reduction for MYPOP-wt PsV treatment (unpublished data of the Florin group). It might therefore be the case that a material deviation attributed the effect to MYPOP-AD alone. More replicates would have been necessary to statistically compensate for the potential material error and thus observe the suspected effect for both preparations. Interestingly, in other transfection experiments, the MYPOP-AD mutant also exhibits a strong growth-inhibitory effect on cancer cells (personal communication with L. Florin), suggesting that MYPOP's function is not solely dependent on DNA binding. It is conceivable that the MYPOP-AD mutant plays a role in an inhibitory complex.

In conclusion, the results of these experiments prompt the question of whether the observed reduction in tumor growth is rather attributable to the combined effect of the entire applied preparation, most likely including the virus capsid itself. The follow-up experiment on lung tumor cells supports this hypothesis. On the one hand, a sole effect of empty PsV on 2427T lung tumor cells was detected. On the other hand, a reduction of cell growth in type A549 lung tumor cells was shown for all three PsV treatments (5.5.2). These findings suggest pseudoviral toxicity, which is consistent with the fact, that viral vectors can induce toxic response mechanisms in targeted cells (Glover, Lipps and Jans, 2005). However, this effect has not yet been explicitly described for HPV-based vectors, which have been successfully applied *in vitro* and *in vivo* (Çuburu *et al.*, 2012; Mitsunaga *et al.*, 2011; Raff *et al.*, 2013). Not entirely in favor of a pseudoviral toxicity hypothesis is the observation that in the follow-up HeLa experiment,

no effect of sole empty PsV was detectable. But as mentioned above, this may also be a statistical problem, for which a larger series of experiments or repetitions would be needed.

Another interesting result is that different tumor cell types responded quite variably to the PsV treatments: In the case of HeLa and lung tumor types 2427T and A549, the PsV treatments caused inhibition of cell counts. However, there was no detectable effect on Siha and 2106T lung tumor cells. Here, the above-mentioned concentration-dependent effect could play a role. It would be conceivable that Siha, for example, at three times the concentration of PsV, would also show inhibited cell growth. This would need to be tested using higher-dose PsV or improving transduction rates. Another possible explanation could be a different binding behavior of the HPV PsV. While tropism towards tumor cells is described for human papillomaviral vectors (Kines *et al.*, 2016), it is also known that requirements of the targeted cell type, such as cell surface heparan sulfate, are necessary (Combita *et al.*, 2001). Thus, it is conceivable that the responses observed in different cell types differ due to interactions of the HPV PsV with the differently equipped cells and their environment.

With respect to normal, non-transformed human cells, the results did not vary. No evidence of toxic effects on cell growth was observed at any tested concentration in either NHEK or primary lung cells. The treatment concentration per cell was comparable at the beginning of each experiment, as care was always taken to seed the same amounts of cells. Nonetheless, the different cell types have distinct velocities of growth. Primary cell types (NHEK and primary lung cells) grow much slower, while Siha are the fastest in doubling their cell counts. Therefore, the concentration of treatment cannot be considered the same throughout. Nevertheless, the applied treatment does not seem toxic for normal cells, because accordingly they experienced even higher concentrations per cell. This is very important in terms of potential therapeutic use. Overall, these findings are consistent with subsequent investigations into the effect of MYPOP mRNA transfection on the transcriptomes of primary and tumor cells: While NHEK cell growth and transcriptome remain unaffected, HeLa cell growth is completely blocked through the downregulation of oncogenes and the upregulation of other tumor suppressors (Strunk *et al.*, 2024).

6.5.3 **Problems in vector-based MYPOP gene transduction**

With IF assays, the transduction of MYPOP was further analyzed. A transduction efficiency of about 44% was estimated (5.4.4). It should be noted that, generally, due to difficulties in detecting cell boundaries in the IF images, signals in the cytoplasm cannot always be accurately assigned to the correct cells. Assuming that the actual transduction efficiency was between 40% and 50%, this would be consistent with the high transduction efficiency typically reported for viral vectors. Depending on vector and targeted cell type, transduction rates

starting from 40% and up to 100% are reported (Verdoodt *et al.*, 2021; Chen, Keiser and Davidson, 2018). For HPV vectors in particular, Peng already speaks of high transduction efficiency in bone marrow cells at a determined rate of 21% *in vitro* (Peng *et al.*, 2010).

No signal was found in the IF assay of cells treated with MYPOP-AD PsV. This was the basis for discovering the defect in the preparation of MYPOP-AD PsV (see section 6.5.1). In contrast, the transduction of MYPOP-wt seemed to have worked due to the corresponding green signals. Especially at higher magnification, however, it is noticeable that the signals are not typical for the expression of the MYPOP protein. The accumulations described in 5.4.5 rather look like a PsV infection pattern, bringing the protein or source of the IF signals along with it. Due to the fact that MYPOP interacts with L2 (Wüstenhagen *et al.*, 2018), it is thinkable that during the production of HPV PsV in HEK cells, MYPOP protein got packaged and therefore is responsible for the signals obtained after transduction. This assumption is supported by subsequent IF assays of the Florin group with MYPOP PsV on A549 and 2106T cells: FLAG-MYPOP colocalized with the HPV L1 protein after transduction, and no FLAG-MYPOP signal was detected in the nucleus of transduced cells (Strunk, 2023). These new results show that not only MYPOP protein is packaged into the HPV PsV, but also that the expression plasmid appears not to be packaged or transcribed in the target cell. It is conceivable that targeted tumor cells degrade or suppress not only endogenous MYPOP but also incoming MYPOP, or suppress its transcription as part of their activated cell growth pathways. Additionally, viral vector-based gene therapy with the MYPOP expression plasmid seems complicated due to MYPOP interactions. This is consistent with the conclusion of Strunk, attributing problems in the PsV preparation to the MYPOP protein as an antiviral factor, likely to interact with the capsid proteins and preventing efficient gene packaging (Strunk, 2023). As MYPOP has been described to comprise general antiviral properties, problems could also occur when using other vector types. Recent studies using adeno-associated viral vectors support this assumption: the application of MYPOP mRNA-specific siRNA during vector production significantly increases the MYPOP vector production rate (personal communication with L. Florin).

These findings suggest that Figure 18 does not show the expression of the constructs in transduced cells, but rather the MYPOP-wt protein that came along with the PsV and MYPOP-AD attached to the cells.

However, since the concept of re-expressing MYPOP as a cancer therapy in tumor cells was successful in Wüstenhagen's initial attempt via pDNA (Wüstenhagen *et al.*, 2018) and has been further supported by successful mRNA transfection recently (Strunk, 2023; Strunk *et al.*, 2024), further research towards *in vivo* application of this promising tumor suppressor should be conducted. The vector-based gene therapy approach in this project was a step in that

direction, but it needs improvement. The results show that following Buck's protocol alone is not sufficient to generate vectors that efficiently induce re-expression of the MYPOP protein in target cells.

6.6 Conclusion and future directions

This project is part of the evolving research field surrounding the still rather unknown tumor suppressor MYPOP. It contributes to a better understanding of its potential clinical role.

Comparison of two polyclonal MYPOP Abs indicated binding to different MYPOP (iso-) forms, which is in line with current research that assumes the coexistence of different post-transcriptionally phosphorylated forms of MYPOP in human cells (Strunk, 2023). The assumption that MYPOP exhibits a phosphorylation-dependent electrophoretic mobility shift could be used in future research to determine *in vivo* levels of phosphorylated MYPOP by polyacrylamide gel electrophoresis-related methods (Lee *et al.*, 2019).

MYPOP mAbs were identified that meet the requirements for reliable application in WB analysis. Following this work, additional validation took place, proving the Abs to be very promising in different research methods (Plath, 2021 and unpublished data of the Florin group). Today, although more manufacturers of polyclonal Abs exist (AviaSystemsBiology, 2024; FisherScientific, 2024), there is still no MYPOP mAb available. The three subclone candidates highlighted in this project could fill this gap in research equipment. Regarding diagnostic applications beyond research, future efforts should focus on MYPOP levels in normal and tumor tissues to determine the potential of MYPOP mAbs as biomarkers.

With regard to the therapeutic use of the tumor suppressor in cancer therapy, important findings were made that highlight problems with the MYPOP application. In the direct application of the purified protein, it became apparent that the elution buffer from the purification process has a cytotoxic effect and would need to be replaced in future experiments. The attempt at MYPOP transduction resulted in the detection of different problems: First, an error occurred in the production of the control virus, which can be avoided by future double testing of both the expressed genes and the capsid proteins in the peak fractions of the PsV preparation. Second, a potential pseudoviral effect on certain tumor cell lines was observed. It needs to be clarified what provokes the decline in cell growth caused by the viral capsid. Since this effect was only observed in tumor cells and not in normal tissues, the results should be further investigated. Finally, it was found that following Buck's protocol without adjustments is not a suitable approach to packaging MYPOP expression plasmid into PsV successfully. The results of this work indicate that the transduced MYPOP was mainly introduced already as a protein by the PsV. This assumption is supported by recent research suggesting that the MYPOP protein itself prevents the effective packaging of its expression plasmid through its

antiviral effect (Strunk, 2023). Nevertheless, the general approach of re-expressing MYPOP therapeutically against cancer remains promising (Wüstenhagen *et al.*, 2018) and is underlined by recent mRNA transfection analyses (Strunk, 2023; Strunk *et al.*, 2024). The pseudoviral approach presented in this work is a step towards *in vivo* application and the results indicate that it does not exert a toxic effect on healthy normal cells. Yet, it would need to be modified and improved. That is why siRNA against the MYPOP protein is currently used during the production of MYPOP-viral vectors to enable efficient packaging of the MYPOP genome (personal communication with L. Florin). Another possible approach would be to use cell-free protocols to produce HPV PsV, preventing MYPOP expression during assembly (Cerqueira *et al.*, 2017; Cerqueira *et al.*, 2016).

In summary, this work presents novel MYPOP mAbs and, therapeutically, makes a contribution towards viral vector-based MYPOP gene therapy through the recognition of key problems.

7 References

Abcam (2023) *Abcam Products [online],* available at: https://www.abcam.com/products/primary-antibodies/mypop-antibody-ab221487.html (Accessed: October 10, 2023).

Adey, A., Burton, J. N., Kitzman, J. O., Hiatt, J. B., Lewis, A. P., Martin, B. K., Qiu, R., Lee, C. and Shendure, J. (2013) 'The haplotype-resolved genome and epigenome of the aneuploid HeLa cancer cell line', *Nature,* 500(7461), pp. 207-11.

Amer, M. H. (2014) 'Gene therapy for cancer: present status and future perspective', *Mol Cell Ther,* 2, pp. 27.

Araldi, R. P., Sant'Ana, T. A., Módolo, D. G., de Melo, T. C., Spadacci-Morena, D. D., de Cassia Stocco, R., Cerutti, J. M. and de Souza, E. B. (2018) 'The human papillomavirus (HPV)-related cancer biology: An overview', *Biomed Pharmacother,* 106, pp. 1537-1556.

Armitage, P. and Doll, R. (1954) 'The age distribution of cancer and a multi-stage theory of carcinogenesis', *Br J Cancer,* 8(1), pp. 1-12.

AviaSystemsBiology (2024) *avia systems biology - products [online],* available at: https://www.avivasysbio.com/mypop-antibody-c-terminal-region-hrp-p100709-p050-hrp.html?srsltid=AfmBOoq8K74HjAILnS2A53pX0W6IMjWkZ7ouIT5zd1-mLaBAnzoTdbap, (Accessed: December 6, 2024).

Baker, T. S., Newcomb, W. W., Olson, N. H., Cowsert, L. M., Olson, C. and Brown, J. C. (1991) 'Structures of bovine and human papillomaviruses. Analysis by cryoelectron microscopy and three-dimensional image reconstruction', *Biophys J,* 60(6), pp. 1445-56.

Bensaad, K. and Vousden, K. H. (2005) 'Savior and slayer: the two faces of p53', *Nat Med,* 11(12), pp. 1278-9.

Bergman, H., Buckley, B. S., Villanueva, G., Petkovic, J., Garritty, C., Lutje, V., Riveros-Balta, A. X., Low, N. and Henschke, N. (2019) 'Comparison of different human papillomavirus (HPV) vaccine types and dose schedules for prevention of HPV-related disease in females and males', *Cochrane Database Syst Rev,* 2019(11).

Bernard, H. U., Burk, R. D., Chen, Z., van Doorslaer, K., zur Hausen, H. and de Villiers, E. M. (2010) 'Classification of papillomaviruses (PVs) based on 189 PV types and proposal of taxonomic amendments', *Virology,* 401(1), pp. 70-9.

Biedenkapp, H., Borgmeyer, U., Sippel, A. E. and Klempnauer, K. H. (1988) 'Viral myb oncogene encodes a sequence-specific DNA-binding activity', *Nature,* 335(6193), pp. 835-7.

Bienkowska-Haba, M., Patel, H. D. and Sapp, M. (2009) 'Target cell cyclophilins facilitate human papillomavirus type 16 infection', *PLoS Pathog,* 5(7), pp. e1000524.

Bienkowska-Haba, M., Williams, C., Kim, S. M., Garcea, R. L. and Sapp, M. (2012) 'Cyclophilins facilitate dissociation of the human papillomavirus type 16 capsid protein L1 from the L2/DNA complex following virus entry', *J Virol,* 86(18), pp. 9875-87.

Bravo, I. G. and Félez-Sánchez, M. (2015) 'Papillomaviruses: Viral evolution, cancer and evolutionary medicine', *Evol Med Public Health,* 2015(1), pp. 32-51.

Buchwalow, I., Samoilova, V., Boecker, W. and Tiemann, M. (2011) 'Non-specific binding of antibodies in immunohistochemistry: fallacies and facts', *Sci Rep,* 1, pp. 28.

Buck, C. B., Day, P. M. and Trus, B. L. (2013) 'The papillomavirus major capsid protein L1', *Virology,* 445(1-2), pp. 169-74.

Buck, C. B., Pastrana, D. V., Lowy, D. R. and Schiller, J. T. (2004) 'Efficient intracellular assembly of papillomaviral vectors', *J Virol,* 78(2), pp. 751-7.

CancerResearchUK (2024) *Cervical cancer statistics [online],* available at https://www.cancerresearchuk.org/health-professional/cancer-statistics/statistics-by-cancer-type/cervical-cancer#heading-Two (Accessed: December 5, 2024).

Carthew, R. W. and Sontheimer, E. J. (2009) 'Origins and Mechanisms of miRNAs and siRNAs', *Cell,* 136(4), pp. 642-55.

Cerqueira, C., Pang, Y. Y., Day, P. M., Thompson, C. D., Buck, C. B., Lowy, D. R. and Schiller, J. T. (2016) 'A Cell-Free Assembly System for Generating Infectious Human Papillomavirus 16 Capsids Implicates a Size Discrimination Mechanism for Preferential Viral Genome Packaging', *J Virol,* 90(2), pp. 1096-107.

Cerqueira, C., Thompson, C. D., Day, P. M., Pang, Y. S., Lowy, D. R. and Schiller, J. T. (2017) 'Efficient Production of Papillomavirus Gene Delivery Vectors in Defined In Vitro Reactions', *Mol Ther Methods Clin Dev,* 5, pp. 165-179.

Chen, Y. H., Keiser, M. S. and Davidson, B. L. (2018) 'Viral Vectors for Gene Transfer', *Curr Protoc Mouse Biol,* 8(4), pp. e58.

Chesson, H. W., Dunne, E. F., Hariri, S. and Markowitz, L. E. (2014) 'The estimated lifetime probability of acquiring human papillomavirus in the United States', *Sex Transm Dis,* 41(11), pp. 660-4.

Choi, Y. H., Chapman, R., Gay, N. and Jit, M. (2012) 'Potential overestimation of HPV vaccine impact due to unmasking of non-vaccine types: quantification using a multi-type mathematical model', *Vaccine,* 30(23), pp. 3383-8.

Combita, A. L., Touzé, A., Bousarghin, L., Sizaret, P. Y., Muñoz, N. and Coursaget, P. (2001) 'Gene transfer using human papillomavirus pseudovirions varies according to virus genotype and requires cell surface heparan sulfate', *FEMS Microbiol Lett,* 204(1), pp. 183-8.

Crawford, L. and Tommasino, M. (1997) 'Oncogenes and antioncogenes in the development of HPV associated tumors', *Clin Dermatol,* 15(2), pp. 207-15.

Çuburu, N., Graham, B. S., Buck, C. B., Kines, R. C., Pang, Y. Y., Day, P. M., Lowy, D. R. and Schiller, J. T. (2012) 'Intravaginal immunization with HPV vectors induces tissue-resident CD8+ T cell responses', *J Clin Invest,* 122(12), pp. 4606-20.

Da Ros, C. T. and Schmitt Cda, S. (2008) 'Global epidemiology of sexually transmitted diseases', *Asian J Androl,* 10(1), pp. 110-4.

Day, P. M., Baker, C. C., Lowy, D. R. and Schiller, J. T. (2004) 'Establishment of papillomavirus infection is enhanced by promyelocytic leukemia protein (PML) expression', *Proc Natl Acad Sci U S A,* 101(39), pp. 14252-7.

de Martel, C., Plummer, M., Vignat, J. and Franceschi, S. (2017) 'Worldwide burden of cancer attributable to HPV by site, country and HPV type', *Int J Cancer,* 141(4), pp. 664-670.

de Villiers, E. M., Fauquet, C., Broker, T. R., Bernard, H. U. and zur Hausen, H. (2004) 'Classification of papillomaviruses', *Virology,* 324(1), pp. 17-27.

DiGiuseppe, S., Bienkowska-Haba, M., Guion, L. G. and Sapp, M. (2017) 'Cruising the cellular highways: How human papillomavirus travels from the surface to the nucleus', *Virus Res,* 231, pp. 1-9.

DiGiuseppe, S., Luszczek, W., Keiffer, T. R., Bienkowska-Haba, M., Guion, L. G. and Sapp, M. J. (2016) 'Incoming human papillomavirus type 16 genome resides in a vesicular compartment throughout mitosis', *Proc Natl Acad Sci U S A,* 113(22), pp. 6289-94.

Doorbar, J. (2013) 'The E4 protein; structure, function and patterns of expression', *Virology,* 445(1-2), pp. 80-98.

Doorbar, J., Egawa, N., Griffin, H., Kranjec, C. and Murakami, I. (2015) 'Human papillomavirus molecular biology and disease association', *Rev Med Virol,* 25 Suppl 1(Suppl Suppl 1), pp. 2-23.

Du, W. W., Qadir, J., Du, K. Y., Chen, Y., Wu, N. and Yang, B. B. (2023) 'Nuclear Actin Polymerization Regulates Cell Epithelial-Mesenchymal Transition', *Adv Sci (Weinh)*, pp. e2300425.

Dubos, C., Stracke, R., Grotewold, E., Weisshaar, B., Martin, C. and Lepiniec, L. (2010) 'MYB transcription factors in Arabidopsis', *Trends Plant Sci,* 15(10), pp. 573-81.

Egawa, N., Nakahara, T., Ohno, S., Narisawa-Saito, M., Yugawa, T., Fujita, M., Yamato, K., Natori, Y. and Kiyono, T. (2012) 'The E1 protein of human papillomavirus type 16 is dispensable for maintenance replication of the viral genome', *J Virol,* 86(6), pp. 3276-83.

Evander, M., Frazer, I. H., Payne, E., Qi, Y. M., Hengst, K. and McMillan, N. A. (1997) 'Identification of the alpha6 integrin as a candidate receptor for papillomaviruses', *J Virol,* 71(3), pp. 2449-56.

Feller, A., Machemer, K., Braun, E. L. and Grotewold, E. (2011) 'Evolutionary and comparative analysis of MYB and bHLH plant transcription factors', *Plant J,* 66(1), pp. 94-116.

Fior R., Z. R. (2019) *Molecular and Cell Biology of Cancer - When Cells Break the Rules and Hijack Their Own Planet [E-Book].* Cham, Switzerland: Springer Nature Switzerland AG, p. 31-93, available at: https://doi.org/10.1007/978-3-030-11812-9

FisherScientific (2024) *Fisher Scientific, part of Thermo Fisher Scientific, products [online],* available at: https://www.fishersci.de/shop/products/mypop-rabbit-anti-human-polyclonal-thermo-scientific-pierce/15969444 (Accessed: December 6, 2024).

Florin, L., Becker, K. A., Lambert, C., Nowak, T., Sapp, C., Strand, D., Streeck, R. E. and Sapp, M. (2006) 'Identification of a dynein interacting domain in the papillomavirus minor capsid protein l2', *J Virol,* 80(13), pp. 6691-6.

Forman, D., de Martel, C., Lacey, C. J., Soerjomataram, I., Lortet-Tieulent, J., Bruni, L., Vignat, J., Ferlay, J., Bray, F., Plummer, M. and Franceschi, S. (2012) 'Global burden of human papillomavirus and related diseases', *Vaccine,* 30 Suppl 5, pp. F12-23.

Friedl, F., Kimura, I., Osato, T. and Ito, Y. (1970) 'Studies on a new human cell line (SiHa) derived from carcinoma of uterus. I. Its establishment and morphology', *Proc Soc Exp Biol Med,* 135(2), pp. 543-5.

Galazka, G., Jurewicz, A., Domowicz, M., Cannella, B., Raine, C. S. and Selmaj, K. (2014) 'HINT1 peptide/Hsp70 complex induces NK-cell-dependent immunoregulation in a model of autoimmune demyelination', *Eur J Immunol,* 44(10), pp. 3026-44.

Gillespie, K. A., Mehta, K. P., Laimins, L. A. and Moody, C. A. (2012) 'Human papillomaviruses recruit cellular DNA repair and homologous recombination factors to viral replication centers', *J Virol,* 86(17), pp. 9520-6.

Gillies, R. J., Didier, N. and Denton, M. (1986) 'Determination of cell number in monolayer cultures', *Anal Biochem,* 159(1), pp. 109-13.

Giroglou, T., Florin, L., Schäfer, F., Streeck, R. E. and Sapp, M. (2001) 'Human papillomavirus infection requires cell surface heparan sulfate', *J Virol,* 75(3), pp. 1565-70.

Glover, D. J., Lipps, H. J. and Jans, D. A. (2005) 'Towards safe, non-viral therapeutic gene expression in humans', *Nat Rev Genet,* 6(4), pp. 299-310.

Guzmán, C., Bagga, M., Kaur, A., Westermarck, J. and Abankwa, D. (2014) 'ColonyArea: an ImageJ plugin to automatically quantify colony formation in clonogenic assays', *PLoS One,* 9(3), pp. e92444.

He, P., Mann-Collura, O., Fling, J., Edara, N., Hetz, R. and Razzaque, M. (2020) 'High phosphate actively induces cytotoxicity by rewiring pro-survival and pro-apoptotic signaling networks in HEK293 and HeLa cells', *The FASEB Journal,* 35(1).

Hu, J., Cao, J., Topatana, W., Juengpanich, S., Li, S., Zhang, B., Shen, J., Cai, L., Cai, X. and Chen, M. (2021) 'Targeting mutant p53 for cancer therapy: direct and indirect strategies', *J Hematol Oncol,* 14(1), pp. 157.

IHRC (2023) *International Human Papillomavirus Reference Center - HPV reference clones [online],* available at: https://www.hpvcenter.se/human_reference_clones/ (Accessed: September 18, 2023).

Isaacson Wechsler, E., Wang, Q., Roberts, I., Pagliarulo, E., Jackson, D., Untersperger, C., Coleman, N., Griffin, H. and Doorbar, J. (2012) 'Reconstruction of human papillomavirus type 16-mediated early-stage neoplasia implicates E6/E7 deregulation and the loss of contact inhibition in neoplastic progression', *J Virol,* 86(11), pp. 6358-64.

Islam, M. S., Chakraborty, B. and Panda, C. K. (2020) 'Human papilloma virus (HPV) profiles in breast cancer: future management', *Ann Transl Med,* 8(10), pp. 650.

Jang, M. K., Shen, K. and McBride, A. A. (2014) 'Papillomavirus genomes associate with BRD4 to replicate at fragile sites in the host genome', *PLoS Pathog,* 10(5), pp. e1004117.

Jeon, S., Allen-Hoffmann, B. L. and Lambert, P. F. (1995) 'Integration of human papillomavirus type 16 into the human genome correlates with a selective growth advantage of cells', *J Virol,* 69(5), pp. 2989-97.

Joyce, J. G., Tung, J. S., Przysiecki, C. T., Cook, J. C., Lehman, E. D., Sands, J. A., Jansen, K. U. and Keller, P. M. (1999) 'The L1 major capsid protein of human papillomavirus type 11 recombinant virus-like particles interacts with heparin and cell-surface glycosaminoglycans on human keratinocytes', *J Biol Chem,* 274(9), pp. 5810-22.

Kalluri, R. and Neilson, E. G. (2003) 'Epithelial-mesenchymal transition and its implications for fibrosis', *J Clin Invest,* 112(12), pp. 1776-84.

Kines, R. C., Cerio, R. J., Roberts, J. N., Thompson, C. D., de Los Pinos, E., Lowy, D. R. and Schiller, J. T. (2016) 'Human papillomavirus capsids preferentially bind and infect tumor cells', *Int J Cancer,* 138(4), pp. 901-11.

Kirnbauer, R., Booy, F., Cheng, N., Lowy, D. R. and Schiller, J. T. (1992) 'Papillomavirus L1 major capsid protein self-assembles into virus-like particles that are highly immunogenic', *Proc Natl Acad Sci U S A,* 89(24), pp. 12180-4.

Klempnauer, K. H., Gonda, T. J. and Bishop, J. M. (1982) 'Nucleotide sequence of the retroviral leukemia gene v-myb and its cellular progenitor c-myb: the architecture of a transduced oncogene', *Cell,* 31(2 Pt 1), pp. 453-63.

Klempnauer, K. H., Ramsay, G., Bishop, J. M., Moscovici, M. G., Moscovici, C., McGrath, J. P. and Levinson, A. D. (1983) 'The product of the retroviral transforming gene v-myb is a truncated version of the protein encoded by the cellular oncogene c-myb', *Cell,* 33(2), pp. 345-55.

Knappe, M., Bodevin, S., Selinka, H. C., Spillmann, D., Streeck, R. E., Chen, X. S., Lindahl, U. and Sapp, M. (2007) 'Surface-exposed amino acid residues of HPV16 L1 protein mediating interaction with cell surface heparan sulfate', *J Biol Chem,* 282(38), pp. 27913-22.

Köhler, G. and Milstein, C. (1975) 'Continuous cultures of fused cells secreting antibody of predefined specificity', *Nature,* 256(5517), pp. 495-7.

Komatsu, T., Nagata, K. and Wodrich, H. (2016) 'The Role of Nuclear Antiviral Factors against Invading DNA Viruses: The Immediate Fate of Incoming Viral Genomes', *Viruses,* 8(10).

Kueng, W., Silber, E. and Eppenberger, U. (1989) 'Quantification of cells cultured on 96-well plates', *Anal Biochem,* 182(1), pp. 16-9.

Lambert, P. F., Münger, K., Rösl, F., Hasche, D. and Tommasino, M. (2020) 'Beta human papillomaviruses and skin cancer', *Nature,* 588(7838), pp. E20-e21.

Lederer, M., Jockusch, B. M. and Rothkegel, M. (2005) 'Profilin regulates the activity of p42POP, a novel Myb-related transcription factor', *J Cell Sci,* 118(Pt 2), pp. 331-41.

Lee, C., 박영하, 김연란, Alan Peterkofsky, /Seok, , 석. and Yeong-Jae (2013) 'Phosphorylation-Dependent Mobility Shift of Proteins on SDS-PAGE is Due to Decreased Binding of SDS', *Bulletin of the Korean Chemical Society,* 34(7), pp. 2063-2066.

Lee, C. R., Park, Y. H., Min, H., Kim, Y. R. and Seok, Y. J. (2019) 'Determination of protein phosphorylation by polyacrylamide gel electrophoresis', *J Microbiol,* 57(2), pp. 93-100.

Major, T., Szarka, K., Sziklai, I., Gergely, L. and Czeglédy, J. (2005) 'The characteristics of human papillomavirus DNA in head and neck cancers and papillomas', *J Clin Pathol,* 58(1), pp. 51-5.

Mandigo, A. C., Tomlins, S. A., Kelly, W. K. and Knudsen, K. E. (2022) 'Relevance of pRB Loss in Human Malignancies', *Clin Cancer Res,* 28(2), pp. 255-264.

McBride, A. A. (2008) 'Replication and partitioning of papillomavirus genomes', *Adv Virus Res,* 72, pp. 155-205.

McBride, A. A. (2013) 'The papillomavirus E2 proteins', *Virology,* 445(1-2), pp. 57-79.

McBride, A. A. (2017) 'Mechanisms and strategies of papillomavirus replication', *Biol Chem,* 398(8), pp. 919-927.

McBride, A. A. (2022) 'Human papillomaviruses: diversity, infection and host interactions', *Nat Rev Microbiol,* 20(2), pp. 95-108.

Mikuličić, S., Strunk, J. and Florin, L. (2021) 'HPV16 Entry into Epithelial Cells: Running a Gauntlet', *Viruses,* 13(12).

Mitsunaga, M., Kosaka, N., Kines, R. C., Roberts, J. N., Lowy, D. R., Schiller, J. T., Ishihara, Y., Hasegawa, A., Choyke, P. L. and Kobayashi, H. (2011) 'In vivo longitudinal imaging of experimental human papillomavirus infection in mice with a multicolor fluorescence mini-endoscopy system', *Cancer Prev Res (Phila),* 4(5), pp. 767-73.

Mukherjee, S. (2010) *The Emperor of all Maladies: A Biography of Cancer [Book].* New York: Scribner, a Division of Simon and Schuster Inc., p. 105 - 234.

Müller, K. H., Spoden, G. A., Scheffer, K. D., Brunnhöfer, R., De Brabander, J. K., Maier, M. E., Florin, L. and Muller, C. P. (2014) 'Inhibition by cellular vacuolar ATPase impairs human papillomavirus uncoating and infection', *Antimicrob Agents Chemother,* 58(5), pp. 2905-11.

Nominé, Y., Masson, M., Charbonnier, S., Zanier, K., Ristriani, T., Deryckère, F., Sibler, A. P., Desplancq, D., Atkinson, R. A., Weiss, E., Orfanoudakis, G., Kieffer, B. and Travé, G. (2006) 'Structural and functional analysis of E6 oncoprotein: insights in the molecular pathways of human papillomavirus-mediated pathogenesis', *Mol Cell,* 21(5), pp. 665-78.

Nordling, C. O. (1953) 'A new theory on cancer-inducing mechanism', *Br J Cancer,* 7(1), pp. 68-72.

Nürnberg, W., Artuc, M., Nawrath, M., Lovric, J., Stüting, S., Moelling, K., Czarnetzki, B. M. and Schadendorf, D. (1995) 'Human c-myb is expressed in cervical carcinomas and transactivates the HPV-16 promoter', *Cancer Res,* 55(19), pp. 4432-7.

Ogata, K., Hojo, H., Aimoto, S., Nakai, T., Nakamura, H., Sarai, A., Ishii, S. and Nishimura, Y. (1992) 'Solution structure of a DNA-binding unit of Myb: a helix-turn-helix-related motif with conserved tryptophans forming a hydrophobic core', *Proc Natl Acad Sci U S A,* 89(14), pp. 6428-32.

patent16/206526 (2020) *patent center uspto [online]*. Application no. US 16/ 206,526 (Florin, Wüstenhagen, Schneider). Available at https:// patentcenter.uspto.gov/applications/16206526 (Accessed: December 6, 2024).

Peng, S., Monie, A., Kang, T. H., Hung, C. F., Roden, R. and Wu, T. C. (2010) 'Efficient delivery of DNA vaccines using human papillomavirus pseudovirions', *Gene Ther,* 17(12), pp. 1453-64.

Plath, M. (2021) *Role of the Myb-related Transcription Factor MYPOP in Cancer Cells [master´s thesis].* Mainz: Medicine of University Medicine Mainz, Biomedicine Studies.

Plotzker, R. E., Vaidya, A., Pokharel, U. and Stier, E. A. (2023) 'Sexually Transmitted Human Papillomavirus: Update in Epidemiology, Prevention, and Management', *Infect Dis Clin North Am,* 37(2), pp. 289-310.

Pünzeler, S., Link, S., Wagner, G., Keilhauer, E. C., Kronbeck, N., Spitzer, R. M., Leidescher, S., Markaki, Y., Mentele, E., Regnard, C., Schneider, K., Takahashi, D., Kusakabe, M., Vardabasso, C., Zink, L. M., Straub, T., Bernstein, E., Harata, M., Leonhardt, H., Mann, M.,

Rupp, R. A. and Hake, S. B. (2017) 'Multivalent binding of PWWP2A to H2A.Z regulates mitosis and neural crest differentiation', *Embo j,* 36(15), pp. 2263-2279.

Pyeon, D., Pearce, S. M., Lank, S. M., Ahlquist, P. and Lambert, P. F. (2009) 'Establishment of human papillomavirus infection requires cell cycle progression', *PLoS Pathog,* 5(2), pp. e1000318.

Raff, A. B., Woodham, A. W., Raff, L. M., Skeate, J. G., Yan, L., Da Silva, D. M., Schelhaas, M. and Kast, W. M. (2013) 'The evolving field of human papillomavirus receptor research: a review of binding and entry', *J Virol,* 87(11), pp. 6062-72.

Rodenhuis, S. and Slebos, R. J. (1992) 'Clinical significance of ras oncogene activation in human lung cancer', *Cancer Res,* 52(9 Suppl), pp. 2665s-2669s.

Rosinski, J. A. and Atchley, W. R. (1998) 'Molecular evolution of the Myb family of transcription factors: evidence for polyphyletic origin', *J Mol Evol,* 46(1), pp. 74-83.

Sakakibara, N., Mitra, R. and McBride, A. A. (2011) 'The papillomavirus E1 helicase activates a cellular DNA damage response in viral replication foci', *J Virol,* 85(17), pp. 8981-95.

Saraiya, M., Unger, E. R., Thompson, T. D., Lynch, C. F., Hernandez, B. Y., Lyu, C. W., Steinau, M., Watson, M., Wilkinson, E. J., Hopenhayn, C., Copeland, G., Cozen, W., Peters, E. S., Huang, Y., Saber, M. S., Altekruse, S. and Goodman, M. T. (2015) 'US assessment of HPV types in cancers: implications for current and 9-valent HPV vaccines', *J Natl Cancer Inst,* 107(6), pp. djv086.

Scheffer, K. D., Berditchevski, F. and Florin, L. (2014) 'The tetraspanin CD151 in papillomavirus infection', *Viruses,* 6(2), pp. 893-908.

Scheffer, K. D., Gawlitza, A., Spoden, G. A., Zhang, X. A., Lambert, C., Berditchevski, F. and Florin, L. (2013) 'Tetraspanin CD151 mediates papillomavirus type 16 endocytosis', *J Virol,* 87(6), pp. 3435-46.

Scheffner, M., Werness, B. A., Huibregtse, J. M., Levine, A. J. and Howley, P. M. (1990) 'The E6 oncoprotein encoded by human papillomavirus types 16 and 18 promotes the degradation of p53', *Cell,* 63(6), pp. 1129-36.

Scheffner, M. and Whitaker, N. J. (2003) 'Human papillomavirus-induced carcinogenesis and the ubiquitin-proteasome system', *Semin Cancer Biol,* 13(1), pp. 59-67.

Schiffman, M., Castle, P. E., Jeronimo, J., Rodriguez, A. C. and Wacholder, S. (2007) 'Human papillomavirus and cervical cancer', *Lancet,* 370(9590), pp. 890-907.

Schirrmacher, V. (2019) 'From chemotherapy to biological therapy: A review of novel concepts to reduce the side effects of systemic cancer treatment (Review)', *Int J Oncol,* 54(2), pp. 407-419.

Schneider, M. A. (2016) *„Identifizierung und Charakterisierung zellulärer Interaktionspartner des minoren Kapsidproteins L2 des Humanen Papillomvirus 16“ [Dissertation].* Mainz: JGU Mainz.

Schwarz, E., Freese, U. K., Gissmann, L., Mayer, W., Roggenbuck, B., Stremlau, A. and zur Hausen, H. (1985) 'Structure and transcription of human papillomavirus sequences in cervical carcinoma cells', *Nature,* 314(6006), pp. 111-4.

Schweiger, L., Lelieveld-Fast, L. A., Mikuličić, S., Strunk, J., Freitag, K., Tenzer, S., Clement, A. M. and Florin, L. (2022) 'HPV16 Induces Formation of Virus-p62-PML Hybrid Bodies to Enable Infection', *Viruses,* 14(7).

Serrano, B., de Sanjosé, S., Tous, S., Quiros, B., Muñoz, N., Bosch, X. and Alemany, L. (2015) 'Human papillomavirus genotype attribution for HPVs 6, 11, 16, 18, 31, 33, 45, 52 and 58 in female anogenital lesions', *Eur J Cancer,* 51(13), pp. 1732-41.

Skelin, J., Sabol, I. and Tomaić, V. (2022) 'Do or Die: HPV E5, E6 and E7 in Cell Death Evasion', *Pathogens,* 11(9).

Spoden, G., Freitag, K., Husmann, M., Boller, K., Sapp, M., Lambert, C. and Florin, L. (2008) 'Clathrin- and caveolin-independent entry of human papillomavirus type 16--involvement of tetraspanin-enriched microdomains (TEMs)', *PLoS One,* 3(10), pp. e3313.

Spoden, G., Kühling, L., Cordes, N., Frenzel, B., Sapp, M., Boller, K., Florin, L. and Schelhaas, M. (2013) 'Human papillomavirus types 16, 18, and 31 share similar endocytic requirements for entry', *J Virol,* 87(13), pp. 7765-73.

Stills, H. (2021) 'Polyclonal Antibody Production', *The Laboratory Rabbit, Guinea Pig, Hamster, and Other Rodents*. London: Elsevier Inc., pp. 259-274.

Strunk, J. (2023) *Characterizing the Myb-related Transcription Factor MYPOP and its Role as Tumor Suppressor [PhD thesis].* Mainz: Johannes Gutenberg University, University Medicine.

Strunk, J., Hüppner, A., Sial, M., Plath, M., Wagner, S., Freitag, K., Mikuličić, S., Bopp, T., Klein, M., Rajalingam, K., Harms, G., Marini, F., Ludt, A., Hankeln, T., Osterhof, C., Henrich, A., Nubbemeyer, A., Suchan, M., Döring, T. and Florin, L. (2024) *The MYB-related transcription factor MYPOP acts as a selective regulator of cancer cell growth.* Research Square.

Syrjänen, K. J. (2002) 'HPV infections and oesophageal cancer', *J Clin Pathol,* 55(10), pp. 721-8.

Szakács, G., Paterson, J. K., Ludwig, J. A., Booth-Genthe, C. and Gottesman, M. M. (2006) 'Targeting multidrug resistance in cancer', *Nat Rev Drug Discov,* 5(3), pp. 219-34.

Tim, B., Kouznetsova, V. L., Kesari, S. and Tsigelny, I. F. (2023) 'Targeting of insulin receptor endocytosis as a treatment to insulin resistance', *J Diabetes Complications,* 37(11), pp. 108615.

Tomasetti, C., Marchionni, L., Nowak, M. A., Parmigiani, G. and Vogelstein, B. (2015) 'Only three driver gene mutations are required for the development of lung and colorectal cancers', *Proc Natl Acad Sci U S A,* 112(1), pp. 118-23.

Uhlen, M., Bandrowski, A., Carr, S., Edwards, A., Ellenberg, J., Lundberg, E., Rimm, D. L., Rodriguez, H., Hiltke, T., Snyder, M. and Yamamoto, T. (2016) 'A proposal for validation of antibodies', *Nat Methods,* 13(10), pp. 823-7.

Van Doorslaer, K. (2013) 'Evolution of the papillomaviridae', *Virology,* 445(1-2), pp. 11-20.

Van Doorslaer, K., Chen, Z., Bernard, H. U., Chan, P. K. S., DeSalle, R., Dillner, J., Forslund, O., Haga, T., McBride, A. A., Villa, L. L., Burk, R. D. and Ictv Report, C. (2018) 'ICTV Virus Taxonomy Profile: Papillomaviridae', *J Gen Virol,* 99(8), pp. 989-990.

Vaquerizas, J. M., Kummerfeld, S. K., Teichmann, S. A. and Luscombe, N. M. (2009) 'A census of human transcription factors: function, expression and evolution', *Nat Rev Genet,* 10(4), pp. 252-63.

Verdoodt, D., Peeleman, N., Van Camp, G., Van Rompaey, V. and Ponsaerts, P. (2021) 'Transduction Efficiency and Immunogenicity of Viral Vectors for Cochlear Gene Therapy: A Systematic Review of Preclinical Animal Studies', *Front Cell Neurosci,* 15, pp. 728610.

Vogelstein, B. and Kinzler, K. W. (2015) 'The Path to Cancer --Three Strikes and You're Out', *N Engl J Med,* 373(20), pp. 1895-8.

Wang, J. W. and Roden, R. B. (2013) 'L2, the minor capsid protein of papillomavirus', *Virology,* 445(1-2), pp. 175-86.

Weichselbaum, R. R. and Kufe, D. (1997) 'Gene therapy of cancer', *Lancet,* 349 Suppl 2, pp. Sii10-2.

WHO (2023) *World Health Organization - Health Topics [online],* available at: https://www.who.int/health-topics/cancer#tab=tab_1 (Accessed: September 28, 2023).

Wood, D. J. and Endicott, J. A. (2018) 'Structural insights into the functional diversity of the CDK-cyclin family', *Open Biol,* 8(9).

Workalemahu, T., Enquobahrie, D. A., Tadesse, M. G., Hevner, K., Gelaye, B., Sanchez, S. E. and Williams, M. A. (2017) 'Genetic variations related to maternal whole blood mitochondrial DNA copy number: a genome-wide and candidate gene study', *J Matern Fetal Neonatal Med,* 30(20), pp. 2433-2439.

Wüstenhagen, E. (2014) *Untersuchungen zur Interaktion des minoren Kapsidproteins L2 des Humanen Papillomvirus Typ 16 mit dem zellulären Transkriptionsfaktor p42POP [master's thesis].* Mainz: Institute of Biology, Johannes Gutenberg-University Mainz.

Wüstenhagen, E. (2017) *A study of human papillomavirus infection: Obscurin-like 1 and MYPOP in HPV entry and transcription [PhD Thesis].* Mainz: Johannes Gutenberg-Universität.

Wüstenhagen, E., Boukhallouk, F., Negwer, I., Rajalingam, K., Stubenrauch, F. and Florin, L. (2018) 'The Myb-related protein MYPOP is a novel intrinsic host restriction factor of oncogenic human papillomaviruses', *Oncogene,* 37(48), pp. 6275-6284.

Xia, X., Wan, R., Wang, P., Huo, W., Dong, H. and Du, Q. (2018) 'Toxicity of imidazoles ionic liquid [C(16)mim]Cl to Hela cells', *Ecotoxicol Environ Saf,* 162, pp. 408-414.

Xu, X., Lai, Y. and Hua, Z. C. (2019) 'Apoptosis and apoptotic body: disease message and therapeutic target potentials', *Biosci Rep,* 39(1).

Yamamoto, A., Kormann, M., Rosenecker, J. and Rudolph, C. (2009) 'Current prospects for mRNA gene delivery', *Eur J Pharm Biopharm,* 71(3), pp. 484-9.

Zhang, C. (2012) 'Hybridoma technology for the generation of monoclonal antibodies', *Methods Mol Biol,* 901, pp. 117-35.

Zhao, K., Bai, X., Wang, X., Cao, Y., Zhang, L., Li, W. and Wang, S. (2023) 'Insight on the hub gene associated signatures and potential therapeutic agents in epilepsy and glioma', *Brain Res Bull,* 199, pp. 110666.

Zhao, K. N., Sun, X. Y., Frazer, I. H. and Zhou, J. (1998) 'DNA packaging by L1 and L2 capsid proteins of bovine papillomavirus type 1', *Virology,* 243(2), pp. 482-91.

Zhou, Y. and Ness, S. A. (2011) 'Myb proteins: angels and demons in normal and transformed cells', *Front Biosci (Landmark Ed),* 16(3), pp. 1109-31.

zur Hausen, H. (1976) 'Condylomata acuminata and human genital cancer', *Cancer Res,* 36(2 pt 2), pp. 794.

zur Hausen, H. (2001) 'Oncogenic DNA viruses', *Oncogene,* 20(54), pp. 7820-3.

zur Hausen, H. (2009) 'Papillomaviruses in the causation of human cancers - a brief historical account', *Virology,* 384(2), pp. 260-5.

Appendix

abcam

Product datasheet

Anti-MYPOP antibody ab94406

1 Image

Overview

Product name	Anti-MYPOP antibody
Description	Rabbit polyclonal to MYPOP
Host species	Rabbit
Tested applications	**Suitable for:** WB
Species reactivity	**Reacts with:** Human **Predicted to work with:** Mouse, Rat, Dog
Immunogen	Synthetic peptide corresponding to a region within N terminal amino acids 72-121 (TGQEVQKRWN DFKRRTKEKL ARVPHSTQGA GPAAEDAFSA EEETIFAILG) of Human MYPOP, NP_001012661 Run BLAST with ExPASy Run BLAST with NCBI
Positive control	COLO205 cell lysate

Properties

Form	Liquid
Storage instructions	Shipped at 4°C. Upon delivery aliquot and store at -20°C. Avoid freeze / thaw cycles.
Storage buffer	Preservative: 0.09% Sodium azide Constituents: 2% Sucrose, PBS
Purity	Immunogen affinity purified
Clonality	Polyclonal
Isotype	IgG

Applications

The Abpromise guarantee Our **Abpromise guarantee** covers the use of ab94406 in the following tested applications.

The application notes include recommended starting dilutions; optimal dilutions/concentrations should be determined by the end user.

Application	Abreviews	Notes

1

Application	Abreviews	Notes
WB		Use a concentration of 1 µg/ml. Predicted molecular weight: 43 kDa. Good results were obtained when blocked with 5% non-fat dry milk in 0.05% PBS-T.

Target

Function	Transcriptional repressor; DNA-binding protein that specifically recognizes the core sequence 5'-YAAC[GT]G-3'. Dimerization with PFN1 reduces its DNA-binding capacity.
Sequence similarities	Contains 1 Myb-like domain.
Domain	The proline-rich region is required for PFN1 interaction.
Cellular localization	Nucleus.

Images

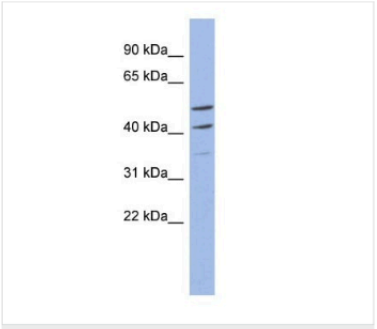

Western blot - Anti-MYPOP antibody (ab94406)

Anti-MYPOP antibody (ab94406) at 1 µg/ml + COLO205 cell lysate at 10 µg

Secondary

HRP conjugated anti-Rabbit IgG

Predicted band size: 43 kDa

Our Abpromise to you: Quality guaranteed and expert technical support

- Replacement or refund for products not performing as stated on the datasheet
- Valid for 12 months from date of delivery
- Response to your inquiry within 24 hours
- We provide support in Chinese, English, French, German, Japanese and Spanish
- Extensive multi-media technical resources to help you
- We investigate all quality concerns to ensure our products perform to the highest standards

If the product does not perform as described on this datasheet, we will offer a refund or replacement. For full details of the Abpromise, please visit **https://www.abcam.com/abpromise** or contact our technical team.

Acknowledgments

I would like to express my sincere appreciation to my doctoral thesis supervisor, for giving me the opportunity to join her group and to realize this exciting project, for thorough feedback and for providing invaluable expertise throughout the research process.

I extend my appreciation to the provider of my scholarship, offering the best support that I can imagine.

I am grateful to all colleagues and group members of the Virology department, who have been a source of inspiration and collaboration.

Lastly, I want to express my heartfelt gratitude to all cherished friends and family who have been a source of laughter, encouragement and understanding during the last years.

Thank you!